Detection of disk-jet coprecession in a tidal disruption event

Citation for the original published paper (version of record):
Wang, Y., Lin, Z., Wu, L. et al (2025). Detection of disk-jet coprecession in a tidal disruption event.
Science advances, 11(50): eady9068-. http://dx.doi.org/10.1126/sciadv.ady9068

(article starts on next page)

SPACE SCIENCES

Detection of disk-jet coprecession in a tidal disruption event

Yanan Wang[1]*†, Zikun Lin[1,2]†, Linhui Wu[3]†, Wei-Hua Lei[4]*, Shuyuan Wei[2], Shuang-Nan Zhang[2,5], Long Ji[6], Santiago del Palacio[7], Ranieri D. Baldi[8], Yang Huang[1,2]*, Ji-Feng Liu[1,2,9,10]*, Bing Zhang[11,12], Aiyuan Yang[1], Ru-Rong Chen[1], Yangwei Zhang[2], Ai-Ling Wang[5], Lei Yang[13], Panos Charalampopoulos[14], David R. A. Williams-Baldwin[15], Zhu-Heng Yao[16], Fu-Guo Xie[3], Defu Bu[17], Hua Feng[5], Xinwu Cao[18], Hongzhou Wu[4], Wenxiong Li[1], Erlin Qiao[1], Giorgos Leloudas[19], Joseph P. Anderson[20,21], Xinwen Shu[13], Dheeraj R. Pasham[22], Hu Zou[1], Matt Nicholl[23], Thomas Wevers[24,25], Tomás E. Müller-Bravo[26,27], Jing Wang[16,28], Jian-Yan Wei[16], Yu-Lei Qiu[16], Wei-Jian Guo[1], Claudia P. Gutiérrez[29,30], Mariusz Gromadzki[31], Cosimo Inserra[32], Lydia Makrygianni[33], Francesca Onori[34], Tanja Petrushevska[35], Diego Altamirano[36], Lluís Galbany[29,30], Miguel Peréz-Torres[37,38], Ting-Wan Chen[39]

Theories and simulations predict that intense space-time curvature near black holes bends the trajectories of light and matter, driving disk and jet precession under relativistic torques. However, direct observational evidence of disk-jet coprecession remains elusive. Here, we report the most compelling case to date: a tidal disruption event (TDE) exhibiting unprecedented 19.6-day quasi-periodic variations in both x-rays and radio, with x-ray amplitudes exceeding an order of magnitude. The nearly synchronized x-ray and radio variations suggest a shared mechanism regulating the emission regions. We demonstrate that a disk-jet Lense-Thirring precession model successfully reproduces these variations while requiring a low-spin black hole. This study uncovers previously uncharted short-term radio variability in TDEs, highlights the transformative potential of high-cadence radio monitoring, and offers profound insights into disk-jet physics.

INTRODUCTION

Tidal disruption events (TDEs) are transient phenomena that occur when a star ventures too close to a supermassive black hole (SMBH) and is torn apart by its tidal forces [e.g., (*1*, *2*)]. The resulting stellar debris falls back toward the SMBH, forming a nascent accretion disk and, in some cases, launching (mildly) relativistic jets [e.g., (*3*–*7*)]. This process unfolds over timescales of months to years, offering a unique opportunity to study accretion and jet-launching physics around SMBHs in real time.

In TDEs, the angular momentum of the accretion disk, imparted by the disrupted star, is often misaligned with the spin axis of the central Kerr black hole (BH). This misalignment is expected to induce Lense-Thirring [LT; (*8*)] precession of the disk and associated jet, driven by frame-dragging effects in the strong-field regime of general relativity [e.g., (*9*, *10*)]. General relativistic magnetohydrodynamic (GRMHD) simulations support this picture, predicting coupled disk-jet precession [e.g., (*11*, *12*)]; however, direct observational confirmation remains elusive. Thus far, disk or jet precession

[1]National Astronomical Observatories, Chinese Academy of Sciences, 20A Datun Road, Beijing 100101, China. [2]School of Astronomy and Space Sciences, University of Chinese Academy of Sciences, Beijing 100049, China. [3]Shanghai Astronomical Observatory, Chinese Academy of Sciences, 80 Nandan Road, Shanghai 200030, China. [4]Department of Astronomy, School of Physics, Huazhong University of Science and Technology, Luoyu Road 1037, Wuhan 430074, China. [5]Key Laboratory of Particle Astrophysics, Institute of High Energy Physics, Chinese Academy of Sciences, 19B Yuquan Road, Beijing 100049, China. [6]School of Physics and Astronomy, Sun Yat-sen University, Zhuhai 519082, China. [7]Department of Space, Earth and Environment, Chalmers University of Technology, SE-412 96 Gothenburg, Sweden. [8]INAF - Istituto di Radioastronomia, Via P. Gobetti 101, I-40129 Bologna, Italy. [9]Institute for Frontiers in Astronomy and Astrophysics, Beijing Normal University, Beijing 102206, China. [10]New Cornerstone Science Laboratory, National Astronomical Observatories, Chinese Academy of Sciences, Beijing 100012, China. [11]The Hong Kong Institute for Astronomy and Astrophysics, University of Hong Kong, Pokfulam Road, Hong Kong, China. [12]Department of Physics, University of Hong Kong, Pokfulam Road, Hong Kong, China. [13]Department of Physics, Anhui Normal University, Wuhu, Anhui 241002, China. [14]Department of Physics and Astronomy, University of Turku, FI-20014 Turku, Finland. [15]Jodrell Bank Centre for Astrophysics, School of Physics and Astronomy, The University of Manchester, Alan Turing Building, Oxford Road, Manchester M13 9PL, UK. [16]Key Laboratory of Space Astronomy and Technology, National Astronomical Observatories, Chinese Academy of Sciences, Beijing 100101, China. [17]Shanghai Key Lab for Astrophysics, Shanghai Normal University, 100 Guilin Road, Shanghai 200234, China. [18]Institute for Astronomy, School of Physics, Zhejiang University, 866 Yuhangtang Road, Hangzhou 310058, China. [19]DTU Space, National Space Institute, Technical University of Denmark, 2800 Kgs. Lyngby, Denmark. [20]European Southern Observatory, Alonso de Córdova 3107, Casilla 19, Santiago, Chile. [21]Millennium Institute of Astrophysics MAS, Nuncio Monsenor Sotero Sanz 100, Off.104, Providencia, Santiago, Chile. [22]Kavli Institute for Astrophysics and Space Research, Massachusetts Institute of Technology, Cambridge, MA 02139, USA. [23]Astrophysics Research Centre, School of Mathematics and Physics, Queens University Belfast, Belfast BT7 1NN, UK. [24]Space Telescope Science Institute, 3700 San Martin Drive, Baltimore, MD 21218, USA. [25]Astrophysics and Space Institute, Schmidt Sciences, New York, NY 10011, USA. [26]School of Physics, Trinity College Dublin, The University of Dublin, Dublin 2, Ireland. [27]Instituto de Ciencias Exactas y Naturales (ICEN), Universidad Arturo Prat, Iquique, Chile. [28]Guangxi Key Laboratory for Relativistic Astrophysics, School of Physical Science and Technology, Guangxi University, Nanning 530004, China. [29]Institut d'Estudis Espacials de Catalunya (IEEC), Edifici RDIT, Campus UPC, 08860 Castelldefels (Barcelona), Spain. [30]Institute of Space Sciences (ICE, CSIC), Campus UAB, Carrer de Can Magrans, s/n, E-08193 Barcelona, Spain. [31]Astronomical Observatory, University of Warsaw, Al. Ujazdowskie 4, 00-478 Warszawa, Poland. [32]Cardiff Hub for Astrophysics Research and Technology, School of Physics and Astronomy, Cardiff University, Queens Buildings, The Parade, Cardiff CF24 3AA, UK. [33]Department of Physics, Lancaster University, Lancaster LA1 4YB, UK. [34]INAF - Osservatorio Astronomico d'Abruzzo via M. Maggini snc, I-64100 Teramo, Italy. [35]Center for Astrophysics and Cosmology, University of Nova Gorica, Vipavska 11c, 5270 Ajdovščina, Slovenia. [36]School of Physics and Astronomy, University of Southampton, Southampton, Hampshire SO17 1BJ, UK. [37]Instituto de Astrofísica de Andalucía (IAA-CSIC), Glorieta de la Astronomía, s/n, E-18008 Granada, Spain. [38]School of Sciences, European University Cyprus, Diogenes Street, Engomi, 1516 Nicosia, Cyprus. [39]Institute of Astronomy, National Central University, 300 Jhongda Road, 32001 Jhongli, Taiwan.
*Corresponding author. Email: wangyn@bao.ac.cn (Y.W.); leiwh@hust.edu.cn (W.-H.L.); huangyang@ucas.ac.cn (Y.H.); jfliu@nao.cas.cn (J.-F.L.)
†These authors contributed equally to this work.

has only been observed separately in various accreting systems, as evidenced by either x-ray [e.g., (*13*–*15*)] or radio observations [e.g., (*16*, *17*)].

The detection of disk-jet coprecession has been impeded by several observational challenges, including the transient nature of the disk and jet, limited cadence in radio monitoring, viewing angle effects, and contamination from other sources of variability. Here, we present the most compelling evidence to date for disk-jet coprecession in a recent TDE, enabled by exceptionally dense temporal coverage in both x-ray and radio observations.

RESULTS

Optical counterpart

AT2020afhd (aka ZTF20abwtifz) is an optical transient situated at the nucleus of the galaxy LEDA 145386 (fig. S1), at a redshift of 0.027 (*18*, *19*). The transient was discovered by the Zwicky Transient Facility (ZTF) in 2020, with initial detections at a *g*-band magnitude of ~20. On 4 January 2024, ZTF detected a substantial rebrightening (*20*), with a peak magnitude of g_{ABmag} ~16.6. Follow-up optical spectra reveal the presence of a blue continuum (consistent with the optical colors of $g - r \sim -0.02$), a He II emission line and broad Balmer emission, leading to the classification of the rebrightening as a TDE (*18*). Moreover, the optical decline rate follows approximately a $t^{-5/3}$ power law (see Fig. 1), consistent with the debris fallback rate predicted by TDE theories (*1*, *2*, *21*). Additionally, we determined the central BH mass using two independent methods (section S5), both of which yielded consistent results. For the subsequent analysis in this work, we adopt a BH mass of $\log(M_{\mathrm{BH}}/M_{\odot}) = 6.7 \pm 0.5$ and take MJD 60310 as the initial date of the rebrightening.

X-ray counterpart

In x-rays, several Neil Gehrels Swift Observatory (Swift) monitoring programs commenced since 26 January 2024 (25 days after the rebrightening). These observations revealed significant variations on timescales of ~25 to 40 days, during which the peak luminosities exceeded the dips by more than one order of magnitude (see Fig. 1). Such variations are also evident in our Neutron star Interior Composition ExploreR (NICER) campaign, triggered 10 days after the initial Swift program. The peak x-ray luminosity is approximately

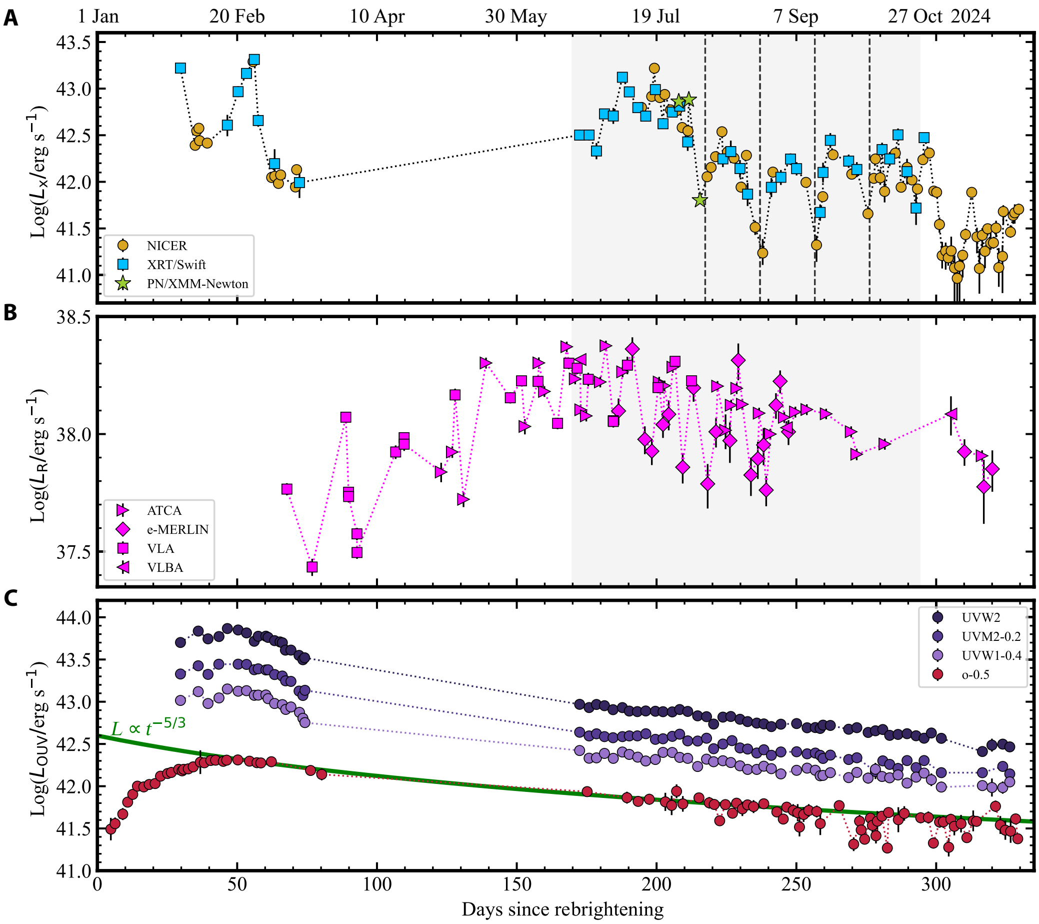

Fig. 1. Temporal evolution of the multiwavelength luminosity of AT2020afhd since its optical rebrightening in 2024 (MJD 60310). (**A**) The unabsorbed x-ray (0.3 to 2 keV) luminosity. (**B**) The radio (5 to 6 GHz) luminosity. The gray-shaded region represents the period used for calculating the cross-correlation function (CCF) between x-ray and radio data. (**C**) The ultraviolet (UV) and optical luminosities. The UltraViolet and Optical Telescope (UVOT) data were corrected for Galactic extinction and had the host contribution subtracted, while the ATLAS data were corrected for extinction. The light curves are offset as indicated in the legend for clarity. The green line indicates a power law of $t^{-5/3}$. Uncertainties are quoted at the 1σ confidence level.

two orders of magnitude higher than in 2020, suggesting that the variations are associated with the newly occurred TDE. Moreover, during the first 300 days, the x-ray spectrum remains ultrasoft, dominated by a multicolor disk blackbody component with $kT_{\text{in}} \sim 10^{5.7-6.4}$ K. The derived blackbody temperature closely follows the evolution of the x-ray luminosity, increasing with rising luminosity and decreasing as it declines (see Fig. 2A).

By 215 days after the rebrightening, the 0.3- to 2-keV x-ray luminosity had dropped by more than an order of magnitude and began exhibiting clear periodic variations, visible to the naked eye. The variation amplitude remained above an order of magnitude. A Lomb-Scargle periodogram (LSP) of background-subtracted x-ray data from 215 to 294 days (3 August to 21 October) identifies a period of 19.6 ± 1.5 days with a statistical significance exceeding 3.79σ (Fig. 3A, see Materials and Methods for details). Notably, the short-term modulation is absent in the high-cadence optical and ultraviolet (UV) photometry. The consistent periodic behavior observed in both the luminosity and blackbody temperature is reminiscent of the TDE AT2020ocn (*15*). In a similar case, AT2020ocn exhibited x-ray modulations with a 15-day period lasting ~130 days, which were attributed to LT precession, although the possibility of radiation-pressure instabilities could not be entirely excluded.

Radio counterpart

In radio bands, AT2020afhd was detected as a point source with the Karl G. Jansky Very Large Array (VLA) 3 days after the first x-ray detection, with a flux density of 253 ± 14 μJy at 15.1 GHz (*22*). The host galaxy of AT2020afhd did not show any past radio activity before the rebrightening. Hence, the nascent radio counterpart is also very likely associated with the TDE. Approximately 67 days later, we initiated high-cadence radio monitoring of AT2020afhd at C band using the VLA, the Australia Telescope Compact Array (ATCA), the Enhanced Multi-Element Remotely Linked Interferometer Network (e-MERLIN), and the Very Long Baseline Array (VLBA). This comprehensive campaign uncovers radio variations with a period of ~20 to 40 days and a peak-to-dip ratio of exceeding four (see Fig. 1). Besides that, we calculated the in-band photon index, $F \propto \nu^{\alpha}$, using VLA and ATCA data and determined the peak frequency, ν_p, and peak flux density, F_p, of the radio broadband spectral energy distribution (SED) using VLA data. Both the long-term increase in the 5-GHz luminosity and the transition of α from positive to negative values suggest that the spectrum evolved from optically thick to optically thin, consistent with the evolution of the SED (see Fig. 2, B and C, and section S3).

Compared to other TDEs with early radio detections (within a hundred days of discovery), AT2020afhd exhibited unprecedented

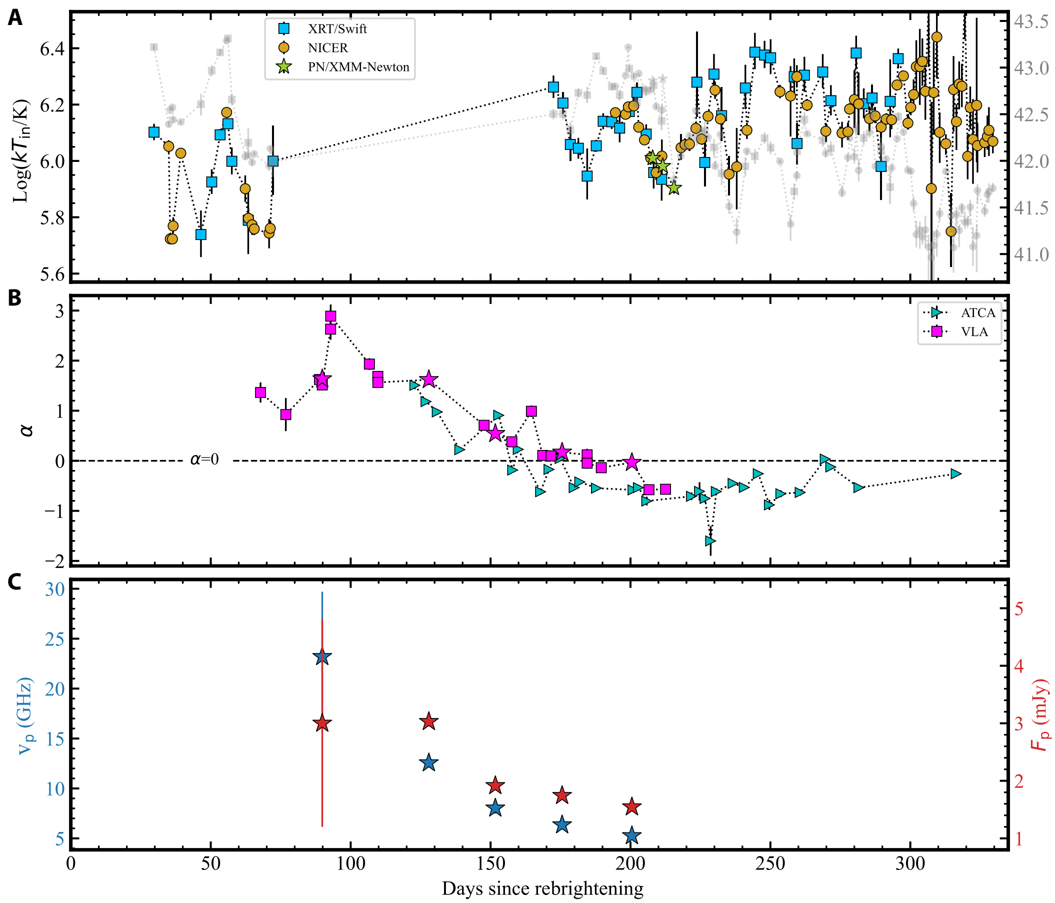

Fig. 2. Temporal evolution of spectral parameters. (**A**) The diskbb temperature derived from x-ray spectra. The luminosity evolution is depicted with gray symbols to illustrate its correlation with temperature; the two parameters generally coevolve, with the temperature reaching its peak alongside luminosity during the first 300 days. (**B**) The in-band spectral index ($F \propto \nu^{\alpha}$) derived from the Very Large Array (VLA; 4 to 8 GHz) and Australia Telescope Compact Array (ATCA; 4 to 10 GHz) data. The stars indicate the VLA observations used for the radio spectral energy distribution (SED) modeling (section S3). (**C**) The peak frequency, ν_p, and the peak flux, F_p, derived from the SED modeling.

high-amplitude variations in radio bands on short-term timescales (as shown in Fig. 4), pointing to the emergence of a previously unidentified class of radio TDEs. Our VLBA U- and C-band observations across different epochs confirmed that the emitting region remained point like (fig. S2). The consistent flux densities observed with VLBA, VLA, and e-MERLIN at similar times indicate that the radio emission, at least at 5 to 6 GHz, originated from a compact, unresolved source, effectively ruling out angular resolution effects. Flux calibration offsets among the VLA, e-MERLIN, and ATCA observations, expected to be up to 22% (section S1.3.5), cannot account for the observed variations. The effect of interstellar scintillation (ISS) (*23*), which would produce hour-scale variations, is excluded

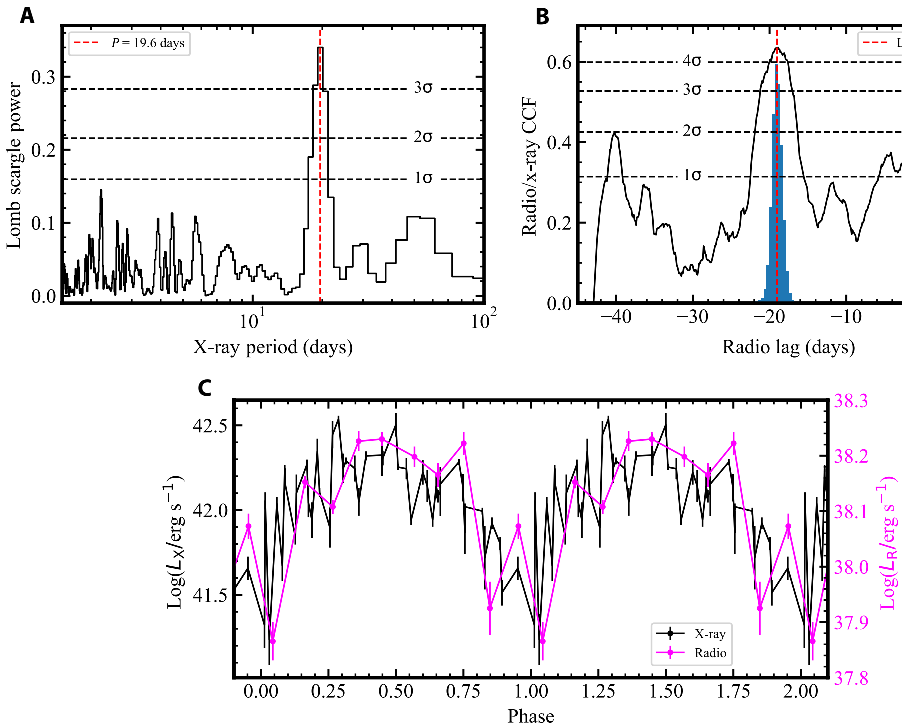

Fig. 3. Timing analysis of the x-ray and radio data. (**A**) Lomb-Scargle periodogram (LSP) of the x-ray light curve. The calculation includes data collected between 3 August and 21 October 2025, during which the x-ray quasi-periodic variations were clearly observed. (**B**) CCF between the x-ray and radio data. The data used in this calculation are indicated by the gray-shaded region in Fig. 1 (A and B). The histogram represents the distribution obtained from bootstrap simulations, with the red dashed line marking the median of the distribution at −19.0 days. (**C**) Folded x-ray and radio light curves with a period of 19.6 days. The radio data were rebinned into 0.1-phase intervals using a weighted mean for clarity. The data used in this calculation are shown in Fig. 5B.

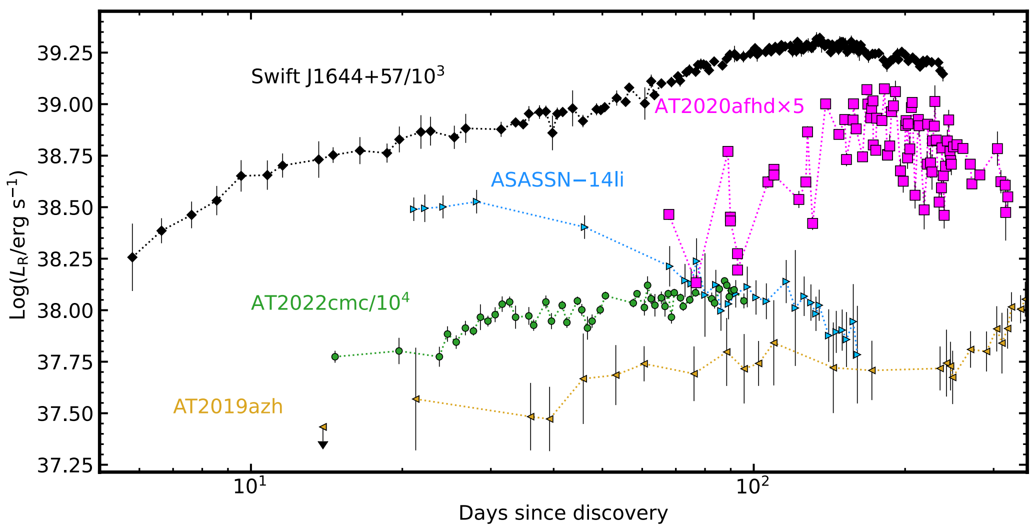

Fig. 4. Comparison of TDEs with early intense radio detection. The luminosities of the two on-axis jetted TDEs, Swift J1644+57 and AT2022cmc, as well as AT2020afhd, have been rescaled for clarity. The AMI-LA data at 15.5 GHz for Swift J1644+57, ASSASN–14li, AT2019azh, and AT2022cmc were adapted from (*54*–*57*), respectively.

on the basis of the consistent flux densities detected in multiple VLA observations taken within 1 hour (Fig. 1B). Emission resulting from winds or jet-wind interactions with the circumnuclear medium is expected to be isotropic and should not exhibit significant modulation on timescales of tens of days. Therefore, the previously uncharted short-term radio variations observed in AT2020afhd are most likely driven by the dynamic evolution of jets.

Cross-correlation between x-ray and radio emission

Unfortunately, the sparse sampling of radio observations, combined with contamination from nonperiodic variations on both long timescales (hundreds of days) and short timescales (days), makes it challenging to directly extract periodicity from the radio data and reliably assess its significance through comprehensive analysis. Instead, we evaluated the connection between x-ray and radio variations using the discrete cross-correlation function [CCF; (*24*), see Materials and Methods]. This analysis revealed a significant 4.26σ correlation between the x-ray and radio emissions, with a primary peak at a time lag of $-19.0^{+0.7}_{-0.6}$ days (Fig. 3, B and C). In addition, two secondary peaks are found at lags of 0 and −40 days, corresponding to integer multiples of the x-ray variability period. These findings suggest that the primary lag of −19 days may result from the limited temporal coverage of the data and noise across different timescales, rather than indicating a definitive physical lead of the radio emission. The nearly synchronized radio and x-ray variations suggest a common mechanism tightly regulating both emissions. The tens-of-day period aligns with disk precession in TDEs (*9*, *10*), making synchronized disk-jet precession the most natural explanation.

Disk-jet coprecession model

To test the disk-jet precession scenario, we first introduced a rigid-body LT precession model under conditions where the accretion rate remained above the Eddington limit during the first year of a TDE involving a SMBH with a mass of $10^{6.7\pm0.5}\ M_\odot$ disrupted a solar-like star. During this period, the disk remains geometrically thick, characterized by a disk angular semithickness $H/R > \alpha$, where α is the disk viscosity parameter (*25*), H is the disk thickness, and R is the disk radius. The disk is assumed to extend from the innermost stable circular orbit (ISCO) to the debris circularization radius (*9*, *10*), and the amplitude of the x-ray variations is attributed to changes in the disk's projected area and periodic obscuration by the outer disk (see Fig. 5A and section S6.1). The BH spin parameter can then be estimated by assuming that the observed period $T_{prec} \sim 19.6$ days corresponds to the LT precession period. Adopting

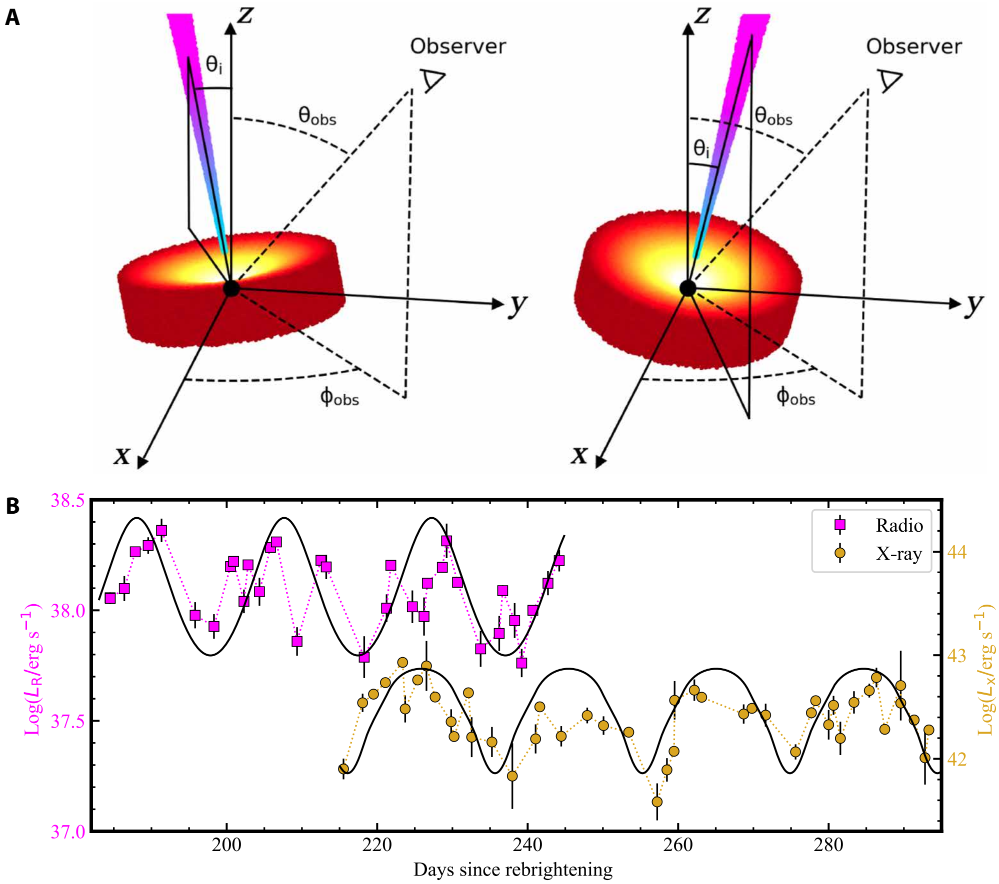

Fig. 5. The disk-jet precession model. (**A**) Schematics of the proposed disk-jet precession model. θ_{obs} and θ_i represent the viewing angle of the system and the disk/jet precession angle around the BH axis, respectively. The left and right plots correspond to the phases of the x-ray and radio variations when the luminosity is relatively low and high, respectively. (**B**) Comparison of the disk-jet precession model (the lower and upper black curves) with x-ray (0.1–2 keV) and radio (5–6 GHz) observations. In the presented model, we adopted a BH mass of $M_\bullet = 10^{6.7} M_\odot$, a scaleheight ratio of $H/R \sim 1$, and an outer disk radius equal to the circularization radius of the debris. As a result, we determined an inclination angle of $\theta_{obs} \sim 37.8 - 38.9°$, a disk/jet precession angle of $\theta_i \sim 14 - 15°$, and a Doppler factor of $\Gamma \sim 1.2 - 1.6$.

several power-law indices for the surface density profile (*10*) and a BH mass range of $M_\bullet = 10^{6.7\pm0.5}\ M_\odot$, we found that the spin parameter $a_\bullet$ fell within the range of $-(0.46\ \text{to}\ 0.14)$ or 0.11 to 0.35 (Fig. 6A). Because a negative spin parameter would result in a larger ISCO and, consequently, a larger inner disk radius, it would be challenging to explain the observed hot disk. Therefore, a positive spin parameter was favored. By modeling the x-ray light curve, we constrained the observer's viewing angle relative to the BH spin to $\theta_{obs} \sim 38.4^{+0.5^\circ}_{-0.6}$ and the disk precession angle to $\theta_i \sim 14.5^\circ \pm 0.5^\circ$ (Fig. 6B).

We then examined the jet precession scenario, in which the radio luminosity varies as the jet cone shifts toward and away from the line of sight. The peak-to-dip ratio is determined by the Doppler factor ratio, which depends on the jet Lorentz factor (Γ) and the

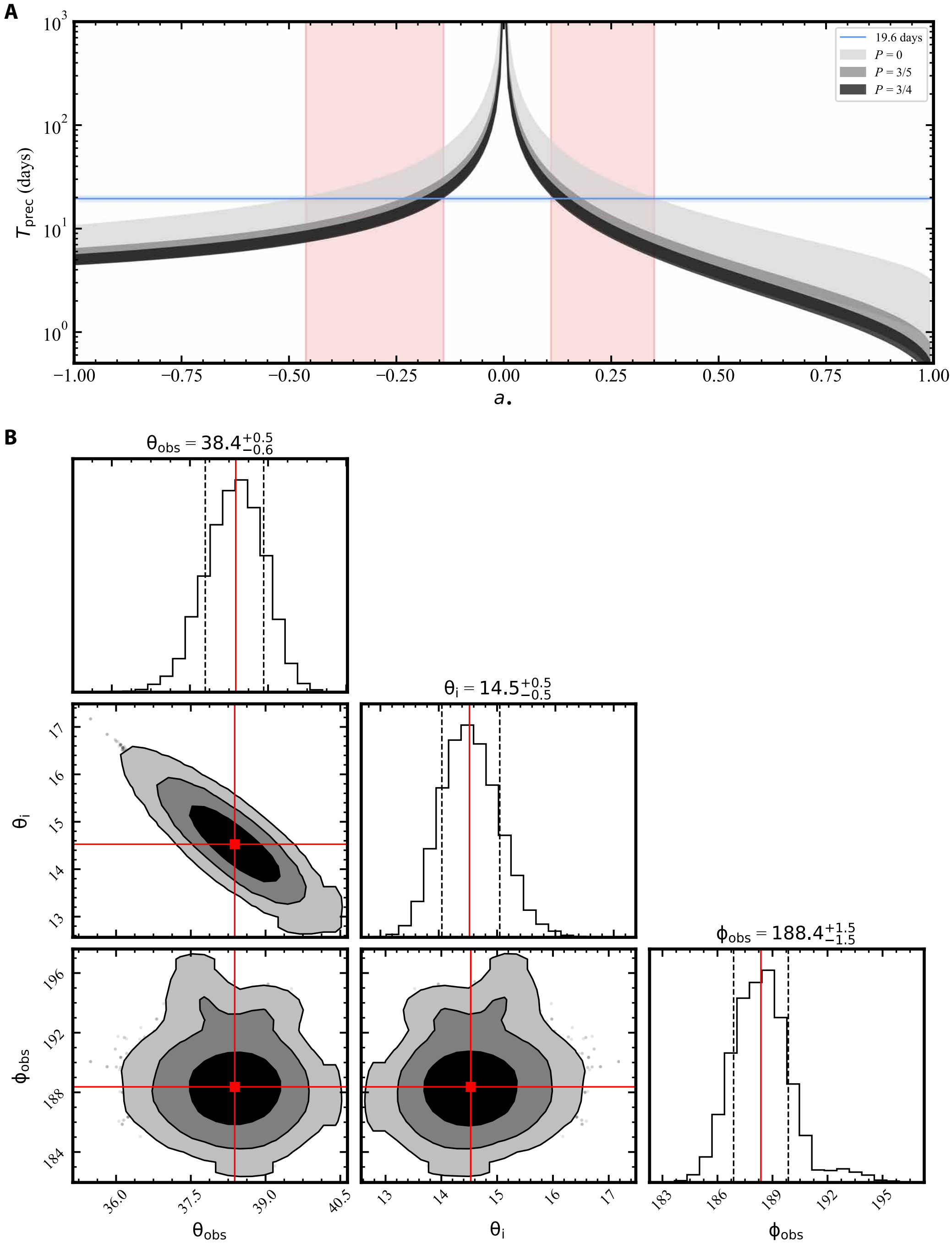

Fig. 6. Estimation of system parameters. (**A**) Disk precession period versus BH spin when adopting various BH masses and surface density profile of the accretion disk. The gray and the blue shades correspond to a BH mass of $10^{6.7\pm0.5}\ M_\odot$ and a period of 19.6 ± 1.5 days. The overlap of the two shades constrains the BH spin to ranges of $-0.46 < a_\bullet < -0.14$ and $0.11 < a_\bullet < 0.35$. (**B**) Contour plots showing the best-fitting parameters for our proposed disk precession model.

angle between the observer and the jet axis (section S6.2). The luminosity peaks when the difference between θ_{obs} and θ_i is minimized and dips when it is maximized. Adopting $\theta_{obs} \sim 38.4°$ and $\theta_i \sim 14.5°$, we derived $1.2 \leq \Gamma \leq 1.6$. Jets can be powered by two primary mechanisms: the Blandford-Znajek [BZ; (*26*)] mechanism, driven by BH spin, and the Blandford-Payne [BP; (*27*)] mechanism, powered by disk rotation. Both mechanisms can account for our radio observations, with the BZ mechanism requiring a stronger magnetic field than the BP mechanism, i.e., $B_\bullet \sim 2.8 \times 10^3$ G for the former and $B_\bullet \sim 1.5 \times 10^3$ G for the latter, assuming a Lorentz factor of $\Gamma = 1.6$. In Fig. 5B, we present a comparison between our disk-jet precession model and the observations.

Around 250 days after the rebrightening, the timescale of radio variations appeared to lengthen, while the x-ray variation profile remained unchanged. After 300 days, the x-ray emission dropped rapidly, and the 19.6-day quasi-periodic variations disappeared. Meanwhile, the radio emission weakened and became anticorrelated with the x-ray emission. Soon after, the UV-optical emission exhibited a second rebrightening, which we exclude from this study to maintain focus. The radio sampling after 250 days is insufficient for detailed tracking of its covariances with x-rays, but the disk-jet connection clearly broke around 300 days. Current GRMHD simulations explore disk-jet coprecession only over limited timescales, predicting a gradual slowdown of both precession and alignment (*11*, *12*). However, when and how this connection breaks, along with the subsequent independent evolution of the components, remain unexplored, warranting future theoretical investigations.

DISCUSSION

Other potential mechanisms driving x-ray and radio covariances

Disk radiation pressure instabilities may also produce comparable periodicity in x-ray and radio emissions. For example, the microquasar GRS 1915+105 exhibited simultaneous periodic modulations in x-ray and radio bands on timescales of 20 to 50 min (*28*–*30*). This periodic flaring activity has been attributed to radiation pressure instabilities, where material in the inner region of an optically thick accretion disk is rapidly depleted and replenished (*31*, *32*). During this process, part of the inner disk is ejected to form a jet, as indicated by a rise in the radio flare coinciding with a dip in the x-ray flare (*28*). However, the x-ray and radio variations in GRS 1915+105 are considerably more complex, resulting in diverse correlations between the two-band light curves (*33*). Overall, the lack of simulations and theoretical models on the short-term evolution of jets during radiation-pressure instabilities makes it challenging to further test this scenario.

Although the correlation between the x-ray and radio variations of AT2020afhd suggests that the latter is unlikely to have an external origin, we investigated the potential effect of ISS (*23*) on our observations. Using the NE2001 model (*34*), we calculated the transition frequency between the strong and weak scintillation regimes to be $\nu_0 = 7.81$ GHz, indicating that our C-band observations (~6 GHz) fall within the strong, refractive scintillation regime. According to (*23*), the modulation index and timescale are given by $m_p = (\nu/\nu_0)^{17/30} = 0.86$ and $t_r = 2(\nu_0/\nu)^{11/5} = 3.6$ hours, respectively. In our VLA dataset, several pairs of observations taken within an hour showed consistent flux densities, indicating that ISS does not significantly contribute to the observed radio variations.

Nature of the 2024 rebrightening

AT2020afhd was initially discovered as an optical transient by the ZTF on 20 October 2020 (*35*). This event could be associated with nuclear activity in the host galaxy (2MASX J0313357–020907), which transitioned from Seyfert II (*36*) to Seyfert I. Supporting evidence includes the evolution of the Hα emission line, which appeared narrow and weak in the 6dF spectrum from 2005, but became broad and prominent in the Dark Energy Spectroscopic Instrument spectrum from 2022, with a measured width of $\sigma = 3298 \pm 81$ km s^{-1}. Additionally, weak x-ray activity was observed, with a luminosity of $10^{41.7\pm0.8}$ erg s^{-1} detected by eROSITA-SRG on 7 February 2020 (fig. S3D). In the radio band, AT2020afhd was not detected in the FIRST 1.4-GHz catalog (with an upper limit of <0.54 mJy beam^{-1}) or in the VLASS survey at 3 GHz during three epochs (November 2017, September 2020, and March 2023). The root mean square noise levels for the individual VLASS observations were ~0.15 mJy beam^{-1}, and the mosaicked image had a sensitivity limit of <0.08 mJy beam^{-1}.

After three and a half years (beginning in 2024), the source showed signs of rebrightening, starting at $g_{AB} \sim 19.5$ on 5 January 2024, peaking at $g_{AB} \sim 16.8$ on 10 February, and then fading to $g_{AB} \sim 18.4$ on 22 December (see fig. S5A). It was initially classified as a TDE by (*18*) based on its persistent blue optical colors, strong UV flux, broad Balmer emission, and broad He II emission. Later, AT2020afhd was reclassified as a Bowen fluorescence flare [BFF; (*19*)], primarily based on the widths of its He II and Balmer emission lines. However, unlike the relatively stable long-term optical, UV, and x-ray emissions observed in BFFs (*37*), AT2020afhd showed a significant decline, nearly 2 magnitudes in UV photometry and more than two orders of magnitude in x-rays, over the course of about a year. Combined with its thermal x-ray spectrum, this behavior aligns more closely with that typically seen in TDEs. Additionally, it remains unclear whether BFFs are triggered by TDEs. We summarized the observation log for the optical spectra with an signal-to-noise ratio greater than 10 in Table 1 and showed the spectra in Fig. 7A. Figure 7B illustrates the evolution of the full width at half maximum (FWHM) of Hα and Hβ, which decreases as the luminosities decrease.

Similar to AT2020ocn (*15*), the optical-UV light curves of AT2020afhd were dominated by a long-term declining trend with no significant short-term variations (see Fig. 1 and fig. S5A), whereas the x-ray and radio photons exhibited high variability on timescales of tens of days. These distinct optical-UV behaviors, compared to radio and x-rays, could be explained by x-ray reprocessing (*38*, *39*) or stream-stream collisions (*40*). In either scenario, the optical-UV emission was produced at a significant distance from the central engine.

In the latest NTT spectrum (27 August 2024, at +239 days), we detected high-ionization coronal lines (CLs). These include Fe XIV λ5303, Fe VII λλ5720, 6087, and Fe X λ6374. There are indications of CLs in the first NTT spectrum taken before the seasonal gap, although they appear substantially weaker. CLs are high-ionization lines (e.g., of iron, neon, argon, and sulfur) that originate from the photoionization or collisional ionization of a clumpy interstellar medium or other preexisting material. Although typically associated with active galactic nuclei (AGN), strong CLs have been detected in the optical spectra of some galaxies that show little to no evidence of AGN activity (*41*, *42*). Many of these CLs have ionization potentials of ≥ 100 eV, requiring a strong extreme UV and/or soft x-ray

Table 1. Summary of the spectroscopic observations.

Epochs	Telescope/instrument	Grism	Observation date (UTC)	Exposure time (s)
4 days	P60/SEDM*	–	2024-01-13T06:00:32	2700
43 days	FLOYDS-S*	–	2024-02-13T10:36:20	1800
55 days	Lijiang 2.4 m/YFOSC	G14@2.5″	2024-02-24T12:16:06	1800
55 days	Lijiang 2.4 m/YFOSC	G8@2.5″	2024-02-24T12:51:50	1800
61 days	Xinglong 2.16 m/BFOSC	G4@1.8″	2024-03-02T11:32:36	3 × 1800
65 days	Xinglong 2.16 m/BFOSC	G4@1.8″	2024-03-06T11:32:32	2 × 1800
73 days	NTT/EFOSC2	G11@1.0″	2024-03-14T00:20:06	1200
239 days	NTT/EFOSC2	G11@1.0″	2024-08-27T09:11:59	1200

*Spectra from P60 and FLOYDS were downloaded directly from the Transient Name Server (www.wis-tns.org/object/2020afhd). The epochs correspond to the times offset from MJD 60310. Spectra with a signal-to-noise ratio below 10 are excluded from the table, as they are not used in the subsequent analysis.

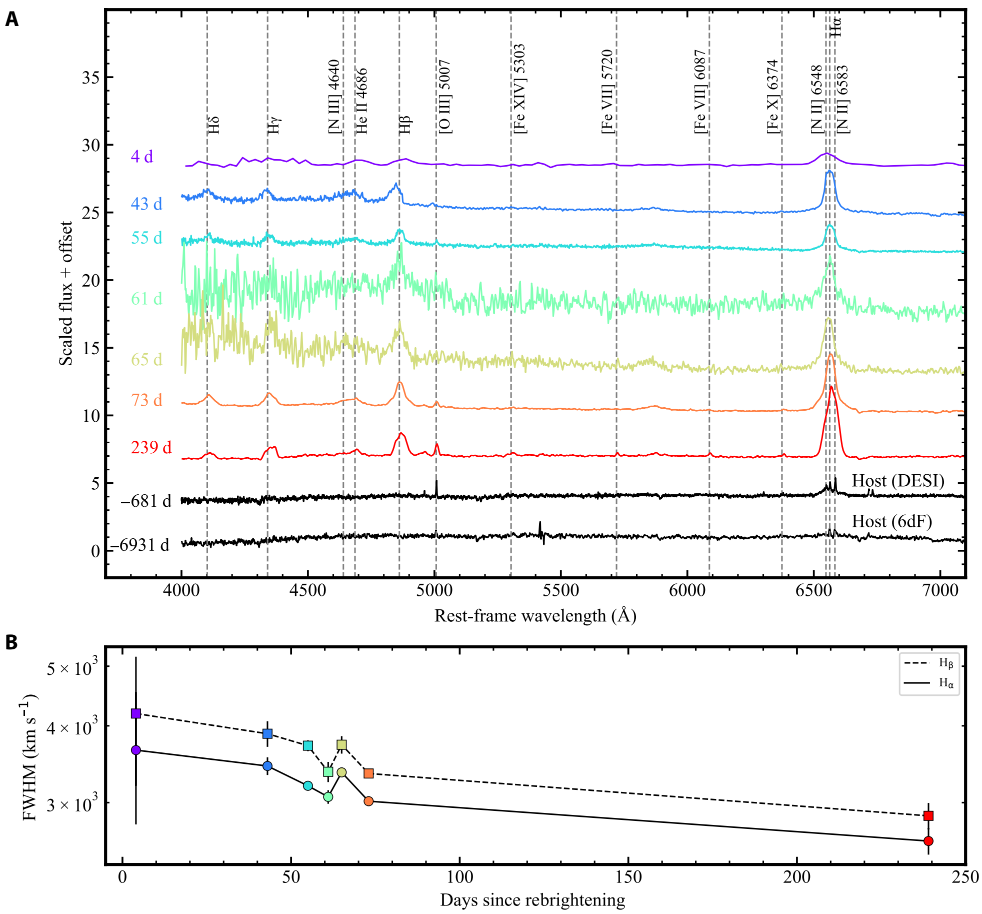

Fig. 7. Optical spectra of AT2020afhd. (**A**) The spectroscopic evolution of AT2020afhd. The spectra have been rescaled and offset for clarity, with rest-frame phases indicated. d, days. (**B**) Evolution of the FWHM of the Hα and Hβ emission lines.

ionizing continuum. It has long been thought that such extreme CL emitters are powered by TDEs, and recent studies support this scenario (*43*, *44*). A few optical-UV TDE candidates (*45*, *46*) out of the ~50 strong candidates discovered to date have exhibited late (≥ 200 days postpeak) x-ray brightening accompanied by the emergence of iron CLs. In contrast, in the case of AT2020afhd, the CLs appear to emerge significantly later than the onset of x-ray emission. Further investigation, including detailed modeling, is required to understand the origin of the CLs, which will be explored in a forthcoming study.

In summary, AT2020afhd exhibits unprecedented high-amplitude, synchronized quasi-periodic variations in x-ray and radio bands, providing the first known evidence that the disk and jet can coprecess on comparable timescales. TDEs, with evolution timescales spanning hundreds of days, serve as unique laboratories for studying the dynamics of nascent accretion disks and jets. Building on the case of AT2020afhd, we propose using modulated x-ray variations as triggers for high-cadence radio follow-ups. This approach aims to efficiently expand the sample of such TDEs and eventually deepen our understanding of disk-jet physics.

MATERIALS AND METHODS

Data summary

AT2020afhd was well detected by both ground- and space-based facilities, with observations spanning from radio to soft x-rays (see the target's localization in fig. S1). Around late November 2024, AT2020afhd exhibited another rebrightening across multiwavelengths at the time of writing. In this study, we focused exclusively on the period between 1 January and 26 November 2024, before the onset of the second rebrightening. Details of the observations, data reduction procedures, and x-ray spectral analysis are provided in sections S1 and S2. We adopted a flat ΛCDM cosmology with $H_0 = 67.4$ km s^{-1} Mpc^{-1} and $\Omega_m = 0.315$ from (*47*), where a redshift of 0.027 corresponds to a luminosity distance of ~123 Mpc.

LSP and CCF

The x-ray light curve was derived from the unabsorbed flux of the diskbb component in the 0.3- to 2-keV band, revealing clear quasi-periodic variations between 3August and 21 October 2024, spanning a total of 79 days. To analyze these variations, we computed the LSP (*48*) using the ASTROPY library (*49*) with data from this 79-day period. To more accurately determine the period of the variations, we divided the NICER observations into individual good time intervals (GTIs) with durations exceeding 300 s. The flux for each NICER GTI was measured following the method described in section S1. Our analysis was performed on a GTI basis for the NICER data and on an observation basis for the x-ray telescope (XRT) and PN data. Given the average sampling interval of 1 day and the total duration of 79 days, we conducted the LSP analysis over a period search range of 1 to 100 days, similar to the range used in the study of AT2020ocn, which had a period of 15 days (*15*). This analysis identified a period of 19.6 days with a FWHM of 3.0 days, as illustrated in the Fig. 3A.

To assess the statistical significance of the detected period, we first quantified the contribution of the LSP continuum by modeling it as a power law, $P(f) \propto f^{\alpha}$. The fit was applied to the observed LSP, excluding the period range corresponding to the detected signal, as defined by its FWHM. The best-fitting power-law index was determined to be $\alpha = -0.02 \pm 0.05$. This value is consistent with 0 within the 1σ uncertainty range, indicating that the continuum was not significantly affected by red noise but was instead dominated by white noise.

To further test whether the continuum was consistent with white noise, we applied the algorithms described in (*50*). We compared the cumulative distribution function (CDF) and probability density function (PDF) of the LSP power values to those expected for white noise. The expected CDF followed $1 - \exp(-z)$ (*48*), where z represented LSP powers. The comparisons of the observed and expected CDF and PDF are shown in Fig. 8 (A and B). To quantify these comparisons, we conducted Kolmogorov-Smirnov (K-S) and

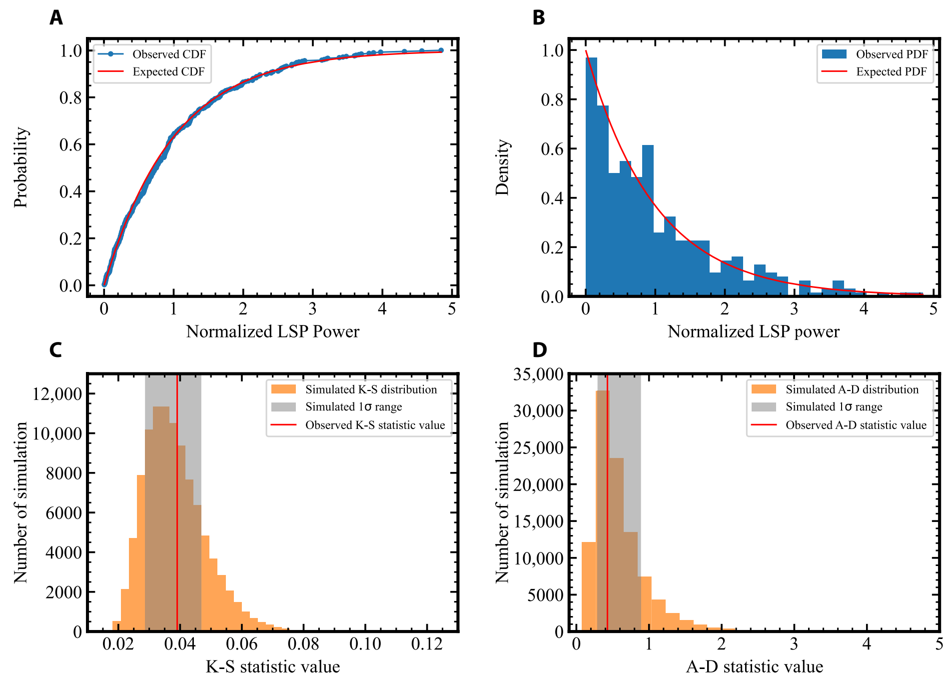

Fig. 8. White noise tests for LSP. (**A**) The CDF of the normalized LSP noise power from the observed data (blue points) compared to the expected CDF of an exponential distribution (red curve). (**B**) The PDF of the normalized LSP noise power from the observed data (blue histogram) compared to the expected PDF of an exponential distribution (red curve). (**C**) Kolmogorov-Smirnov (K-S) test results from simulations. The orange histogram shows the distribution of K-S statistic values for simulated white noise, with the 1σ range shaded in gray. The red line represents the K-S statistic value for the observed LSP noise power. (**D**) Anderson-Darling (A-D) goodness-of-fit test results from simulations. The orange histogram shows the distribution of A-D statistic values for simulated white noise, with the 1σ range shaded in gray. The red line represents the A-D statistic value for the observed LSP noise power.

Anderson-Darling (A-D) goodness-of-fit tests on the observed and expected CDF using the SCIPY library (*51*). The K-S test yielded a statistic of 0.0391 ($P = 0.93$), and the A-D test returned a statistic of 0.4278, which is well below the 10% critical value of 1.07. These results indicate that, at a 90% confidence level, the null hypothesis that the LSP power followed the expected white noise distribution could not be rejected. Additionally, we performed 100,000 Monte Carlo simulations of the LSP continuum under the assumption of white noise and computed their corresponding K-S and A-D statistics. The distributions of these statistics are presented in Fig. 8 (C and D). The K-S and A-D statistic values of the observed CDF fell within the 1σ range of the distribution of the simulated white noise statistic values. These findings robustly indicated that the LSP continuum was statistically consistent with white noise.

To determine the global statistical significance of the period, we conducted a false alarm probability analysis. We generated 100,000 simulated light curves with the same temporal sampling as the observed data, allowing the flux values to vary randomly within the observed range, bounded by the minimum and maximum flux. From these simulations, we identified 15 occurrences of spurious periodic signals, corresponding to a statistical significance of ~3.79σ.

To investigate the correlation between radio and x-ray variations of AT2020afhd, we used the Python-based discrete CCF (*24*), focusing on data collected between 19 June and 21 October 2024. The analysis revealed that the CCF peaked at a time lag of ~−19.0 days (see Fig. 3B). To assess the global significance of this correlation, we generated 100,000 random radio light curves, preserving the same observation sampling while randomizing the luminosities within the observed minimum and maximum values. We tested the CCF across time lags spanning −45 to 10 days, a range covering ±1 cycle of the periodic signal. Among these simulations, only two spurious CCF signals were detected, corresponding to a statistical significance of ~4.26σ. Furthermore, we estimated the uncertainties in the time lag by focusing on the range of −30 to −10 days, corresponding to a single period cycle around the CCF peak. Using 100,000 Monte Carlo simulations with a bin size of 0.1 days and bootstrapping methods to estimate uncertainties (*24*, *52*), we determined a time lag of $-19.0^{+0.7}_{-0.6}$ days for the radio relative to the x-ray. This result is consistent with the observed period, indicating that the x-ray and radio emissions were synchronized. As described in section S1.3.5, we applied a 22% offset to the observed ATCA flux density. Using the original ATCA flux density and following the same methodology outlined above, we obtained a statistical significance of 3.85σ and a time lag of $-19.1^{+0.6}_{-0.7}$ days. These results indicate that the calibration offset had no substantial impact on the derived time lag or the statistical significance of the correlation.

Additionally, we folded the x-ray and radio light curves with a 19.6-day period. For clarity, the folded radio light curve was rebinned into 0.1-phase intervals using a weighted mean, with error estimation described in (*53*). The folded x-ray and rebinned radio light curves are shown in Fig. 3C.

Supplementary Materials

This PDF file includes:
Sections S1 to S6
Figs. S1 to S5
References

REFERENCES AND NOTES

1. M. J. Rees, Tidal disruption of stars by black holes of 10^6–10^8 solar masses in nearby galaxies. *Nature* **333**, 523–528 (1988).
2. C. R. Evans, C. S. Kochanek, The tidal disruption of a star by a massive black hole. *Astrophys. J.* **346**, L13 (1989).
3. A. J. Levan, N. R. Tanvir, S. B. Cenko, D. A. Perley, K. Wiersema, J. S. Bloom, A. S. Fruchter, A. D. U. Postigo, P. T. O'Brien, N. Butler, A. J. van der Horst, G. Leloudas, A. N. Morgan, K. Misra, G. C. Bower, J. Farihi, R. L. Tunnicliffe, M. Modjaz, J. M. Silverman, J. Hjorth, C. Thöne, A. Cucchiara, J. M. C. Cerón, A. J. Castro-Tirado, J. A. Arnold, M. Bremer, J. P. Brodie, T. Carroll, M. C. Cooper, P. A. Curran, R. M. Cutri, J. Ehle, D. Forbes, J. Fynbo, J. Gorosabel, J. Graham, D. I. Hoffman, S. Guziy, P. Jakobsson, A. Kamble, T. Kerr, M. M. Kasliwal, C. Kouveliotou, D. Kocevski, N. M. Law, P. E. Nugent, E. O. Ofek, D. Poznanski, R. M. Quimby, E. Rol, A. J. Romanowsky, R. Sánchez-Ramírez, S. Schulze, N. Singh, L. van Spaandonk, R. L. C. Starling, R. G. Strom, J. C. Tello, O. Vaduvescu, P. J. Wheatley, R. A. M. J. Wijers, J. M. Winters, D. Xu, An extremely luminous panchromatic outburst from the nucleus of a distant galaxy. *Science* **333**, 199–202 (2011).
4. J. S. Bloom, D. Giannios, B. D. Metzger, S. B. Cenko, D. A. Perley, N. R. Butler, N. R. Tanvir, A. J. Levan, P. T. O'Brien, L. E. Strubbe, F. de Colle, E. Ramirez-Ruiz, W. H. Lee, S. Nayakshin, E. Quataert, A. R. King, A. Cucchiara, J. Guillochon, G. C. Bower, A. S. Fruchter, A. N. Morgan, A. J. van der Horst, A possible relativistic jetted outburst from a massive black hole fed by a tidally disrupted star. *Science* **333**, 203–206 (2011).
5. S. B. Cenko, H. A. Krimm, A. Horesh, A. Rau, D. A. Frail, J. A. Kennea, A. J. Levan, S. T. Holland, N. R. Butler, R. M. Quimby, J. S. Bloom, A. V. Filippenko, A. Gal-Yam, J. Greiner, S. R. Kulkarni, E. O. Ofek, F. Olivares E, P. Schady, J. M. Silverman, N. R. Tanvir, D. Xu, Swift J2058.4+0516: Discovery of a possible second relativistic tidal disruption flare? *Astrophys. J.* **753**, 77 (2012).
6. G. C. Brown, A. J. Levan, E. R. Stanway, N. R. Tanvir, S. B. Cenko, E. Berger, R. Chornock, A. Cucchiaria, Swift J1112.2–8238: A candidate relativistic tidal disruption flare. *Mon. Not. R. Astron. Soc.* **452**, 4297–4306 (2015).
7. I. Andreoni, M. W. Coughlin, D. A. Perley, Y. Yao, W. Lu, S. B. Cenko, H. Kumar, S. Anand, A. Y. Q. Ho, M. M. Kasliwal, A. de Ugarte Postigo, A. Sagués-Carracedo, S. Schulze, D. A. Kann, S. R. Kulkarni, J. Sollerman, N. Tanvir, A. Rest, L. Izzo, J. J. Somalwar, D. L. Kaplan, T. Ahumada, G. C. Anupama, K. Auchettl, S. Barway, E. C. Bellm, V. Bhalerao, J. S. Bloom, M. Bremer, M. Bulla, E. Burns, S. Campana, P. Chandra, P. Charalampopoulos, J. Cooke, V. D'Elia, K. K. das, D. Dobie, J. F. A. Fernández, J. Freeburn, C. Fremling, S. Gezari, S. Goode, M. J. Graham, E. Hammerstein, V. R. Karambelkar, C. D. Kilpatrick, E. C. Kool, M. Krips, R. R. Laher, G. Leloudas, A. Levan, M. J. Lundquist, A. A. Mahabal, M. S. Medford, M. C. Miller, A. Möller, K. P. Mooley, A. J. Nayana, G. Nir, P. T. H. Pang, E. Paraskeva, R. A. Perley, G. Petitpas, M. Pursiainen, V. Ravi, R. Ridden-Harper, R. Riddle, M. Rigault, A. C. Rodriguez, B. Rusholme, Y. Sharma, I. A. Smith, R. D. Stein, C. Thöne, A. Tohuvavohu, F. Valdes, J. van Roestel, S. D. Vergani, Q. Wang, J. Zhang, A very luminous jet from the disruption of a star by a massive black hole. *Nature* **612**, 430–434 (2022).
8. J. Lense, H. Thirring, Über den einfluß der eigenrotation der zentralkörper auf die bewegung der planeten und monde nach der Einsteinschen gravitationstheorie. *Physikalische Zeitschrift* **19**, 156 (1918).
9. N. Stone, A. Loeb, Observing Lense-Thirring precession in tidal disruption flares. *Phys. Rev. Lett.* **108**, 061302 (2012).
10. A. Franchini, G. Lodato, S. Facchini, Lense-Thirring precession around supermassive black holes during tidal disruption events. *Mon. Not. R. Astron. Soc.* **455**, 1946–1956 (2016).
11. M. Liska, C. Hesp, A. Tchekhovskoy, A. Ingram, M. van der Klis, S. Markoff, Formation of precessing jets by tilted black hole discs in 3D general relativistic MHD simulations. *Mon. Not. R. Astron. Soc.* **474**, L81–L85 (2018).
12. K. Chatterjee, Z. Younsi, M. Liska, A. Tchekhovskoy, S. B. Markoff, D. Yoon, D. van Eijnatten, C. Hesp, A. Ingram, M. B. M. van der Klis, Observational signatures of disc and jet misalignment in images of accreting black holes. *Mon. Not. R. Astron. Soc.* **499**, 362–378 (2020).
13. C. J. Saxton, R. Soria, K. Wu, N. P. M. Kuin, Long-term X-ray variability of Swift J1644+57. *Mon. Not. R. Astron. Soc.* **422**, 1625–1639 (2012).
14. X. Ma, L. Tao, S. N. Zhang, L. Zhang, Q. C. Bu, M. Y. Ge, Y. P. Chen, J. L. Qu, S. Zhang, F. J. Lu, L. M. Song, Y. J. Yang, F. Yuan, C. Cai, X. L. Cao, Z. Chang, G. Chen, L. Chen, T. X. Chen, Y. B. Chen, Y. Chen, W. Cui, W. W. Cui, J. K. Deng, Y. W. Dong, Y. Y. du, M. X. Fu, G. H. Gao, H. Gao, M. Gao, Y. D. Gu, J. Guan, C. C. Guo, D. W. Han, Y. Huang, J. Huo, L. Ji, S. M. Jia, L. H. Jiang, W. C. Jiang, J. Jin, Y. J. Jin, L. D. Kong, B. Li, C. K. Li, G. Li, M. S. Li, T. P. Li, W. Li, X. Li, X. B. Li, X. F. Li, Y. G. Li, Z. W. Li, X. H. Liang, J. Y. Liao, B. S. Liu, C. Z. Liu, G. Q. Liu, H. W. Liu, X. J. Liu, Y. N. Liu, B. Lu, X. F. Lu, Q. Luo, T. Luo, B. Meng, Y. Nang, J. Y. Nie, G. Ou, N. Sai, R. C. Shang, X. Y. Song, L. Sun, Y. Tan, Y. L. Tuo, C. Wang, G. F. Wang, J. Wang, L. J. Wang, W. S. Wang, Y. S. Wang, X. Y. Wen, B. Y. Wu, B. B. Wu, M. Wu, G. C. Xiao, S. Xiao, F. G. Xie, S. L. Xiong, H. Xu, Y. P. Xu, J. W. Yang, S. Yang, Y. J. Yang, Q. B. Yi, Q. Q. Yin, Y. You, A. M. Zhang, C. M. Zhang, F. Zhang, H. M. Zhang, J. Zhang, T. Zhang, W. C. Zhang, W. Zhang, W. Z. Zhang, Y. Zhang, Y. F. Zhang, Y. J. Zhang, Y. Zhang, Z. Zhang, Z. Zhang, Z. L. Zhang, H. S. Zhao, X. F. Zhao, S. J. Zheng, D. K. Zhou, J. F. Zhou, Y. X. Zhu, Y. Zhu,

R. L. Zhuang, Discovery of oscillations above 200 keV in a black hole X-ray binary with Insight-HXMT. *Nat. Astron.* **5**, 94–102 (2021).
15. D. R. Pasham, M. Zajaček, C. J. Nixon, E. R. Coughlin, M. Śniegowska, A. Janiuk, B. Czerny, T. Wevers, M. Guolo, Y. Ajay, M. Loewenstein, Lense-Thirring precession after a supermassive black hole disrupts a star. *Nature* **630**, 325–328 (2024).
16. Y. Cui, K. Hada, T. Kawashima, M. Kino, W. Lin, Y. Mizuno, H. Ro, M. Honma, K. Yi, J. Yu, J. Park, W. Jiang, Z. Shen, E. Kravchenko, J. C. Algaba, X. Cheng, I. Cho, G. Giovannini, M. Giroletti, T. Jung, R. S. Lu, K. Niinuma, J. Oh, K. Ohsuga, S. Sawada-Satoh, B. W. Sohn, H. R. Takahashi, M. Takamura, F. Tazaki, S. Trippe, K. Wajima, K. Akiyama, T. An, K. Asada, S. Buttaccio, D. Y. Byun, L. Cui, Y. Hagiwara, T. Hirota, J. Hodgson, N. Kawaguchi, J. Y. Kim, S. S. Lee, J. W. Lee, J. A. Lee, G. Maccaferri, A. Melis, A. Melnikov, C. Migoni, S. J. Oh, K. Sugiyama, X. Wang, Y. Zhang, Z. Chen, J. Y. Hwang, D. K. Jung, H. R. Kim, J. S. Kim, H. Kobayashi, B. Li, G. Li, X. Li, Z. Liu, Q. Liu, X. Liu, C. S. Oh, T. Oyama, D. G. Roh, J. Wang, N. Wang, S. Wang, B. Xia, H. Yan, J. H. Yeom, Y. Yonekura, J. Yuan, H. Zhang, R. Zhao, W. Zhong, Precessing jet nozzle connecting to a spinning black hole in M87. *Nature* **621**, 711–715 (2023).
17. P. Tian, P. Zhang, W. Wang, P. Wang, X. Sun, J. Liu, B. Zhang, Z. Dai, F. Yuan, S. Zhang, Q. Liu, P. Jiang, X. Wu, Z. Zheng, J. Chen, D. Li, Z. Zhu, Z. Pan, H. Gan, X. Chen, N. Sai, Subsecond periodic radio oscillations in a microquasar. *Nature* **621**, 271–275 (2023).
18. E. Hammerstein, R. Chornock, S. Gezari, Y. Yao, "ZTF transient classification report for 2024-02-03" (Transient Name Server, Classification Report 2024-336, 2024).
19. I. Arcavi, S. Faris, M. Newsome, M. Sniegowska, B. Trakhtenbrot, "Re-classification of AT 2020afhd as a Bowen fluorescence flare at z=0.027" (Transient Name Server, AstroNote 53, 2024).
20. C. Fremling, "ZTF transient discovery report for 2024-01-13" (Transient Name Server, Discovery Report 2024-135, 2024).
21. E. S. Phinney, "Manifestations of a massive black hole in the galactic center," in *The Center of the Galaxy*, M. Morris, Ed., vol. 136 of *IAU Symposium* (Springer, 1989), p. 543.
22. C. T. Christy, K. D. Alexander, N. Franz, W. W. Golay, S. Gezari, T. Laskar, T. Eftekhari, D. R. Pasham, M. Pérez-Torres, Y. Cendes, J. Miller-Jones, Radio detection of the nuclear transient AT2020afhd/ZTF20abwtifz. *TNS AstroNote* **56**, 1 (2024).
23. M. A. Walker, Interstellar scintillation of compact extragalactic radio sources. *Mon. Not. R. Astron. Soc.* **294**, 307–311 (1998).
24. M. Sun, C. J. Grier, B. M. Peterson, "PyCCF: Python cross correlation function for reverberation mapping studies" (Astrophysics Source Code Library, record ascl:1805.032, 2018).
25. N. I. Shakura, R. A. Sunyaev, Black holes in binary systems. Observational appearance. *Astron. Astrophys.* **24**, 337–355 (1973).
26. R. D. Blandford, R. L. Znajek, Electromagnetic extraction of energy from Kerr black holes. *Mon. Not. R. Astron. Soc.* **179**, 433–456 (1977).
27. R. D. Blandford, D. G. Payne, Hydromagnetic flows from accretion discs and the production of radio jets. *Mon. Not. R. Astron. Soc.* **199**, 883–903 (1982).
28. G. G. Pooley, R. P. Fender, The variable radio emission from GRS 1915+=105. *Mon. Not. R. Astron. Soc.* **292**, 925–933 (1997).
29. I. F. Mirabel, V. Dhawan, S. Chaty, L. F. Rodriguez, J. Marti, C. R. Robinson, J. Swank, T. Geballe, Accretion instabilities and jet formation in GRS 1915+105. *Astron. Astrophys.* **330**, L9–L12 (1998).
30. F. M. Vincentelli, J. Neilsen, A. J. Tetarenko, Y. Cavecchi, N. C. Segura, S. del Palacio, J. van den Eijnden, G. Vasilopoulos, D. Altamirano, M. A. Padilla, C. D. Bailyn, T. Belloni, D. J. K. Buisson, V. A. Cúneo, N. Degenaar, C. Knigge, K. S. Long, F. Jiménez-Ibarra, J. Milburn, T. M. Darias, M. Ö. Arabacı, R. Remillard, T. Russell, A shared accretion instability for black holes and neutron stars. *Nature* **615**, 45–49 (2023).
31. T. Belloni, M. Méndez, A. R. King, M. van der Klis, J. van Paradijs, An unstable central disk in the superluminal black hole X-ray binary GRS 1915+105. *Astrophys. J.* **479**, L145–L148 (1997).
32. T. Belloni, M. Méndez, A. R. King, M. van der Klis, J. van Paradijs, A unified model for the spectral variability in GRS 1915+105. *Astrophys. J.* **488**, L109–L112 (1997).
33. M. Klein-Wolt, R. P. Fender, G. G. Pooley, T. Belloni, S. Migliari, E. H. Morgan, M. van der Klis, Hard X-ray states and radio emission in GRS 1915+105. *Mon. Not. R. Astron. Soc.* **331**, 745–764 (2002).
34. J. M. Cordes, T. J. W. Lazio, NE2001.I. A new model for the galactic distribution of free electrons and its fluctuations. arXiv:astro-ph/0207156 (2002).
35. E. C. Bellm, S. R. Kulkarni, M. J. Graham, R. Dekany, R. M. Smith, R. Riddle, F. J. Masci, G. Helou, T. A. Prince, S. M. Adams, C. Barbarino, T. Barlow, J. Bauer, R. Beck, J. Belicki, R. Biswas, N. Blagorodnova, D. Bodewits, B. Bolin, V. Brinnel, T. Brooke, B. Bue, M. Bulla, R. Burruss, S. B. Cenko, C.-K. Chang, A. Connolly, M. Coughlin, J. Cromer, V. Cunningham, K. De, A. Delacroix, V. Desai, D. A. Duev, G. Eadie, T. L. Farnham, M. Feeney, U. Feindt, D. Flynn, A. Franckowiak, S. Frederick, C. Fremling, A. Gal-Yam, S. Gezari, M. Giomi, D. A. Goldstein, V. Z. Golkhou, A. Goobar, S. Groom, E. Hacopians, D. Hale, J. Henning, A. Y. Q. Ho, D. Hover, J. Howell, T. Hung, D. Huppenkothen, D. Imel, W.-H. Ip, Ž. Ivezić, E. Jackson, L. Jones, M. Juric, M. M. Kasliwal, S. Kaspi, S. Kaye, M. S. P. Kelley, M. Kowalski, E. Kramer, T. Kupfer, W. Landry, R. R. Laher, C.-D. Lee, H. W. Lin, Z.-Y. Lin, R. Lunnan, M. Giomi, A. Mahabal, P. Mao, A. A. Miller, S. Monkewitz, P. Murphy, C.-C. Ngeow, J. Nordin, P. Nugent, E. Ofek, M. T. Patterson, B. Penprase, M. Porter, L. Rauch, U. Rebbapragada, D. Reiley, M. Rigault, H. Rodriguez, J. van Roestel, B. Rusholme, J. van Santen, S. Schulze, D. L. Shupe, L. P. Singer, M. T. Soumagnac, R. Stein, J. Surace, J. Sollerman, P. Szkody, F. Taddia, S. Terek, A. Van Sistine, S. van Velzen, W. T. Vestrand, R. Walters, C. Ward, Q.-Z. Ye, P.-C. Yu, L. Yan, J. Zolkowe, The Zwicky Transient Facility: System overview, performance, and first results. *Publ. Astron. Soc. Pac.* **131**, 018002 (2019).
36. Y.-P. Chen, I. Zaw, G. R. Farrar, S. Elgamal, A uniformly selected, southern-sky 6dF, optical AGN catalog. *Astrophys. J. Suppl. Ser.* **258**, 29 (2022).
37. B. Trakhtenbrot, I. Arcavi, C. Ricci, S. Tacchella, D. Stern, H. Netzer, P. G. Jonker, A. Horesh, J. E. Mejía-Restrepo, G. Hosseinzadeh, V. Hallefors, D. A. Howell, C. McCully, M. Baloković, M. Heida, N. Kamraj, G. B. Lansbury, Ł. Wyrzykowski, M. Gromadzki, A. Hamanowicz, S. B. Cenko, D. J. Sand, E. Y. Hsiao, M. M. Phillips, T. R. Diamond, E. Kara, K. C. Gendreau, Z. Arzoumanian, R. Remillard, A new class of flares from accreting supermassive black holes. *Nat. Astron.* **3**, 242–250 (2019).
38. J. Guillochon, E. Ramirez-Ruiz, Hydrodynamical simulations to determine the feeding rate of black holes by the tidal disruption of stars: The importance of the impact parameter and stellar structure. *Astrophys. J.* **767**, 25 (2013).
39. N. Roth, D. Kasen, J. Guillochon, E. Ramirez-Ruiz, The X-ray through optical fluxes and line strengths of tidal disruption events. *Astrophys. J.* **827**, 3 (2016).
40. C. Bonnerot, W. Lu, Simulating disc formation in tidal disruption events. *Mon. Not. R. Astron. Soc.* **495**, 1374–1391 (2020).
41. S. Komossa, H. Zhou, T. Wang, M. Ajello, J. Ge, J. Greiner, H. Lu, M. Salvato, R. Saxton, H. Shan, D. Xu, W. Yuan, Discovery of superstrong, fading, iron line emission and double-peaked Balmer lines of the galaxy SDSS J095209.56+214313.3: The light echo of a huge flare. *Astrophys. J.* **678**, L13–L16 (2008).
42. T.-G. Wang, H. Y. Zhou, S. Komossa, H. Y. Wang, W. Yuan, C. Yang, Extreme coronal line emitters: Tidal disruption of stars by massive black holes in galactic nuclei? *Astrophys. J.* **749**, 115 (2012).
43. J. T. Hinkle, B. J. Shappee, T. W. S. Holoien, Coronal line emitters are tidal disruption events in gas-rich environments. *Mon. Not. R. Astron. Soc.* **528**, 4775–4784 (2024).
44. P. Clark, O. Graur, J. Callow, J. Aguilar, S. Ahlen, J. P. Anderson, E. Berger, T. E. Müller-Bravo, T. G. Brink, D. Brooks, T.-W. Chen, T. Claybaugh, A. de la Macorra, P. Doel, A. V. Filippenko, J. E. Forero-Romero, S. Gomez, M. Gromadzki, K. Honscheid, C. Inserra, T. Kisner, M. Landriau, L. Makrygianni, M. Manera, A. Meisner, R. Miquel, J. Moustakas, M. Nicholl, J. Nie, F. Onori, A. Palmese, C. Poppett, T. Reynolds, M. Rezaie, G. Rossi, E. Sanchez, M. Schubnell, G. Tarlé, B. A. Weaver, T. Wevers, D. R. Young, W. K. Zheng, Z. Zhou, Long-term follow-up observations of extreme coronal line emitting galaxies. *Mon. Not. R. Astron. Soc.* **528**, 7076–7102 (2024).
45. F. Onori, G. Cannizzaro, P. G. Jonker, M. Kim, M. Nicholl, S. Mattila, T. M. Reynolds, M. Fraser, T. Wevers, E. Brocato, J. P. Anderson, R. Carini, P. Charalampopoulos, P. Clark, M. Gromadzki, C. P. Gutiérrez, N. Ihanec, C. Inserra, A. Lawrence, G. Leloudas, P. Lundqvist, T. E. Müller-Bravo, S. Piranomonte, M. Pursiainen, K. A. Rybicki, A. Somero, D. R. Young, K. C. Chambers, H. Gao, T. J. L. de Boer, E. A. Magnier, The nuclear transient AT 2017gge: A tidal disruption event in a dusty and gas-rich environment and the awakening of a dormant SMBH. *Mon. Not. R. Astron. Soc.* **517**, 76–98 (2022).
46. P. Short, A. Lawrence, M. Nicholl, M. Ward, T. M. Reynolds, S. Mattila, C. Yin, I. Arcavi, A. Carnall, P. Charalampopoulos, M. Gromadzki, P. G. Jonker, S. Kim, G. Leloudas, I. Mandel, F. Onori, M. Pursiainen, S. Schulze, C. Villforth, T. Wevers, Delayed appearance and evolution of coronal lines in the TDE AT2019qiz. *Mon. Not. R. Astron. Soc.* **525**, 1568–1587 (2023).
47. Planck Collaboration, Planck 2018 results. VI. Cosmological parameters. *Astron. Astrophys.* **641**, A6 (2020).
48. J. D. Scargle, Studies in astronomical time series analysis. II. Statistical aspects of spectral analysis of unevenly spaced data. *Astrophys. J.* **263**, 835–853 (1982).
49. Ice Cube collaboration, R. Abbasi, Y. Abdou, M. Ackermann, J. Adams, J. A. Aguilar, M. Ahlers, D. Altmann, K. Andeen, J. Auffenberg, X. Bai, M. Baker, S. W. Barwick, V. Baum, R. Bay, K. Beattie, J. J. Beatty, S. Bechet, J. B. Tjus, K.-H. Becker, M. Bell, M. L. Benabderrahmane, S. B. Zvi, J. Berdermann, P. Berghaus, D. Berley, E. Bernardini, D. Bertrand, D. Z. Besson, D. Bindig, M. Bissok, E. Blaufuss, J. Blumenthal, D. J. Boersma, C. Bohm, D. Bose, S. Böser, O. Botner, L. Brayeur, A. M. Brown, R. Bruijn, J. Brunner, S. Buitink, M. Carson, J. Casey, M. Casier, D. Chirkin, B. Christy, F. Clevermann, S. Cohen, D. F. Cowen, A. H. C. Silva, M. Danninger, J. Daughhetee, J. C. Davis, C. De Clercq, F. Descamps, P. Desiati, G. de Vries Uiterweerd, T. De Young, J. C. Díaz-Vélez, J. Dreyer, J. P. Dumm, M. Dunkman, R. Eagan, J. Eisch, R. W. Ellsworth, O. Engdegård, S. Euler, P. A. Evenson, O. Fadiran, A. R. Fazely, A. Fedynitch, J. Feintzeig, T. Feusels, K. Filimonov, C. Finley, T. Fischer-Wasels, S. Flis, A. Franckowiak, R. Franke, K. Frantzen, T. Fuchs, T. K. Gaisser, J. Gallagher, L. Gerhardt, L. Gladstone, T. Glüsenkamp, A. Goldschmidt, J. A. Goodman, D. Góra, D. Grant, A. Groß, S. Grullon, M. Gurtner, C. Ha, A. H. Ismail, A. Hallgren, F. Halzen, K. Hanson, D. Heereman, P. Heimann, D. Heinen, K. Helbing, R. Hellauer, S. Hickford, G. C. Hill, K. D. Hoffman, R. Hoffmann, A. Homeier, K. Hoshina, W. Huelsnitz, P. O. Hulth, K. Hultqvist, S. Hussain, A. Ishihara, E. Jacobi, J. Jacobsen,

G. S. Japaridze, O. Jlelati, A. Kappes, T. Karg, A. Karle, J. Kiryluk, F. Kislat, J. Kläs, S. R. Klein, J.-H. Köhne, G. Kohnen, H. Kolanoski, L. Köpke, C. Kopper, S. Kopper, D. J. Koskinen, M. Kowalski, M. Krasberg, G. Kroll, J. Kunnen, N. Kurahashi, T. Kuwabara, M. Labare, K. Laihem, H. Landsman, M. J. Larson, R. Lauer, M. Lesiak-Bzdak, J. Lünemann, J. Madsen, R. Maruyama, K. Mase, H. S. Matis, F. M. Nally, K. Meagher, M. Merck, P. Mészáros, T. Meures, S. Miarecki, E. Middell, N. Milke, J. Miller, L. Mohrmann, T. Montaruli, R. Morse, S. M. Movit, R. Nahnhauer, U. Naumann, S. C. Nowicki, D. R. Nygren, A. Obertacke, S. Odrowski, A. Olivas, M. Olivo, A. O'Murchadha, S. Panknin, L. Paul, J. A. Pepper, C. P. de los Heros, D. Pieloth, N. Pirk, J. Posselt, P. B. Price, G. T. Przybylski, L. Rädel, K. Rawlins, P. Redl, E. Resconi, W. Rhode, M. Ribordy, M. Richman, B. Riedel, J. P. Rodrigues, F. Rothmaier, C. Rott, T. Ruhe, B. Ruzybayev, D. Ryckbosch, S. M. Saba, T. Salameh, H.-G. Sander, M. Santander, S. Sarkar, K. Schatto, M. Scheel, F. Scheriau, T. Schmidt, M. Schmitz, S. Schoenen, S. Schöneberg, L. Schönherr, A. Schönwald, A. Schukraft, L. Schulte, O. Schulz, D. Seckel, S. H. Seo, Y. Sestayo, S. Seunarine, M. W. E. Smith, M. Soiron, D. Soldin, G. M. Spiczak, C. Spiering, M. Stamatikos, T. Stanev, A. Stasik, T. Stezelberger, R. G. Stokstad, A. Stößl, E. A. Strahler, R. Ström, G. W. Sullivan, H. Taavola, I. Taboada, A. Tamburro, S. Ter-Antonyan, S. Tilav, P. A. Toale, S. Toscano, M. Usner, D. van der Drift, N. van Eijndhoven, A. Van Overloop, J. van Santen, M. Vehring, M. Voge, C. Walck, T. Waldenmaier, M. Wallraff, M. Walter, R. Wasserman, C. Weaver, C. Wendt, S. Westerhoff, N. Whitehorn, K. Wiebe, C. H. Wiebusch, D. R. Williams, H. Wissing, M. Wolf, T. R. Wood, K. Woschnagg, C. Xu, D. L. Xu, X. W. Xu, J. P. Yanez, G. Yodh, S. Yoshida, P. Zarzhitsky, J. Ziemann, A. Zilles, M. Zoll, Searches for high-energy neutrino emission in the galaxy with the combined icecube-amanda detector. *Astrophys. J.* **763**, 18 (2013).

50. D. R. Pasham, F. Tombesi, P. Suková, M. Zajaček, S. Rakshit, E. Coughlin, P. Kosec, V. Karas, M. Masterson, A. Mummery, T. W. S. Holoien, M. Guolo, J. Hinkle, B. Ripperda, V. Witzany, B. Shappee, E. Kara, A. Horesh, S. van Velzen, I. Sfaradi, D. Kaplan, N. Burger, T. Murphy, R. Remillard, J. F. Steiner, T. Wevers, R. Arcodia, J. Buchner, A. Merloni, A. Malyali, A. Fabian, M. Fausnaugh, T. Daylan, D. Altamirano, A. Payne, E. C. Ferraraa, A case for a binary black hole system revealed via quasi-periodic outflows. *Sci. Adv.* **10**, eadj8898 (2024).
51. P. Virtanen, R. Gommers, T. E. Oliphant, M. Haberland, T. Reddy, D. Cournapeau, E. Burovski, P. Peterson, W. Weckesser, J. Bright, S. J. van der Walt, M. Brett, J. Wilson, K. J. Millman, N. Mayorov, A. R. J. Nelson, E. Jones, R. Kern, E. Larson, C. J. Carey, İ. Polat, Y. Feng, E. W. Moore, J. V. Plas, D. Laxalde, J. Perktold, R. Cimrman, I. Henriksen, E. A. Quintero, C. R. Harris, A. M. Archibald, A. H. Ribeiro, F. Pedregosa, P. van Mulbregt, SciPy 1.0 Contributors, SciPy 1.0: Fundamental algorithms for scientific computing in Python. *Nat. Methods* **17**, 261–272 (2020).
52. B. M. Peterson, I. Wanders, K. Horne, S. Collier, T. Alexander, S. Kaspi, D. Maoz, On uncertainties in cross-correlation lags and the reality of wavelength-dependent continuum lags in active galactic nuclei. *Publ. Astron. Soc. Pac.* **110**, 660–670 (1998).
53. M. R. Standing, L. Sairam, D. V. Martin, A. H. M. J. Triaud, A. C. M. Correia, G. A. L. Coleman, T. A. Baycroft, V. Kunovac, I. Boisse, A. C. Cameron, G. Dransfield, J. P. Faria, M. Gillon, N. C. Hara, C. Hellier, J. Howard, E. Lane, R. Mardling, P. F. L. Maxted, N. J. Miller, R. P. Nelson, J. A. Orosz, F. Pepe, A. Santerne, D. Sebastian, S. Udry, W. F. Welsh, Radial-velocity discovery of a second planet in the TOI-1338/BEBOP-1 circumbinary system. *Nat. Astron.* **7**, 702–714 (2023).
54. E. Berger, A. Zauderer, G. G. Pooley, A. M. Soderberg, R. Sari, A. Brunthaler, M. F. Bietenholz, Radio monitoring of the tidal disruption event swift J164449.3+573451. I. Jet energetics and the pristine parsec-scale environment of a supermassive black hole. *Astrophys. J.* **748**, 36 (2012).
55. J. S. Bright, R. P. Fender, S. E. Motta, K. Mooley, Y. C. Perrott, S. van Velzen, S. Carey, J. Hickish, N. Razavi-Ghods, D. Titterington, P. Scott, K. Grainge, A. Scaife, T. Cantwell, C. Rumsey, Long-term radio and X-ray evolution of the tidal disruption event ASASSN-14li. *Mon. Not. R. Astron. Soc.* **475**, 4011–4019 (2018).
56. I. Sfaradi, A. Horesh, R. Fender, D. A. Green, D. R. A. Williams, J. Bright, S. Schulze, A late-time radio flare following a possible transition in accretion state in the tidal disruption event AT 2019azh. *Astrophys. J.* **933**, 176 (2022).
57. L. Rhodes, J. S. Bright, R. Fender, I. Sfaradi, D. A. Green, A. Horesh, K. Mooley, D. Pasham, S. Smartt, D. J. Titterington, A. J. van der Horst, D. R. A. Williams, Day-time-scale variability in the radio light curve of the Tidal Disruption Event AT2022cmc: Confirmation of a highly relativistic outflow. *Mon. Not. R. Astron. Soc.* **521**, 389–395 (2023).
58. P. W. A. Roming, T. E. Kennedy, K. O. Mason, J. A. Nousek, L. Ahr, R. E. Bingham, P. S. Broos, M. J. Carter, B. K. Hancock, H. E. Huckle, S. D. Hunsberger, H. Kawakami, R. Killough, T. S. Koch, M. K. Mc Lelland, K. Smith, P. J. Smith, J. C. Soto, P. T. Boyd, A. A. Breeveld, S. T. Holland, M. Ivanushkina, M. S. Pryzby, M. D. Still, J. Stock, The swift ultra-violet/optical telescope. *Space Sci. Rev.* **120**, 95–142 (2005).
59. A. N. Heinze, J. L. Tonry, L. Denneau, H. Flewelling, B. Stalder, A. Rest, K. W. Smith, S. J. Smartt, H. Weiland, A first catalog of variable stars measured by the Asteroid Terrestrial-impact Last Alert System (ATLAS). *Astrophys. J.* **156**, 241 (2018).
60. J. L. Tonry, L. Denneau, A. N. Heinze, B. Stalder, K. W. Smith, S. J. Smartt, C. W. Stubbs, H. J. Weiland, A. Rest, ATLAS: A high-cadence all-sky survey system. *Publ. Astron. Soc. Pac.* **130**, 064505 (2018).
61. L. Shingles, K. W. Smith, D. R. Young, S. J. Smartt, J. Tonry, L. Denneau, A. Heinze, H. Weiland, H. Flewelling, B. Stalder, A. Clocchiatti, F. Förster, G. Pignata, A. Rest, J. Anderson, C. Stubbs, N. Erasmus, "Release of the ATLAS Forced Photometry server for public use" (Transient Name Server AstroNote 7, 2021).
62. J. Wei, B. Cordier, S. Antier, P. Antilogus, J-L. Atteia, A. Bajat, S. Basa, V. Beckmann, M. G. Bernardini, S. Boissier, L. Bouchet, V. Burwitz, A. Claret, Z-G. Dai, F. Daigne, J. Deng, D. Dornic, H. Feng, T. Foglizzo, H. Gao, N. Gehrels, O. Godet, A. Goldwurm, F. Gonzalez, L. Gosset, D. Götz, C. Gouiffes, F. Grise, A. Gros, J. Guilet, X. Han, M. Huang, Y-F. Huang, M. Jouret, A. Klotz, O. L. Marle, C. Lachaud, E. L. Floch, W. Lee, N. Leroy, L-X. Li, S. C. Li, Z. Li, E-W. Liang, H. Lyu, K. Mercier, G. Migliori, R. Mochkovitch, P. O'Brien, J. Osborne, J. Paul, E. Perinati, P. Petitjean, F. Piron, Y. Qiu, A. Rau, J. Rodriguez, S. Schanne, N. Tanvir, E. Vangioni, S. Vergani, F-Y. Wang, J. Wang, X-G. Wang, X-Y. Wang, A. Watson, N. Webb, J. J. Wei, R. Willingale, C. Wu, X-F. Wu, L-P. Xin, D. Xu, S. Yu, W-F. Yu, Y-W. Yu, B. Zhang, S-N. Zhang, Y. Zhang, X. L. Zhou, The deep and transient universe in the SVOM Era: New challenges and opportunities - Scientific prospects of the SVOM mission. arXiv:1610.06892 (2016).
63. D. Tody, "The IRAF data reduction and analysis system," in *Instrumentation in Astronomy VI*, D. L. Crawford, Ed., vol. 627 of *Society of Photo-Optical Instrumentation Engineers (SPIE) Conference Series* (SPIE, 1986), p. 733.
64. D. Tody, "IRAF in the nineties," in *Astronomical Data Analysis Software and Systems II*, R. J. Hanisch, R. J. V. Brissenden, and Jeannette Barnes, Eds. (Astronomical Society of the Pacific, 1993), vol. 52, p. 173.
65. B. Buzzoni, B. Delabre, H. Dekker, S. Dodorico, D. Enard, P. Focardi, B. Gustafsson, W. Nees, J. Paureau, R. Reiss, The ESO faint object spectrograph and camera (EFOSC). *ESO Messenger* **38**, 9 (1984).
66. S. J. Smartt, S. Valenti, M. Fraser, C. Inserra, D. R. Young, M. Sullivan, A. Pastorello, S. Benetti, A. Gal-Yam, C. Knapic, M. Molinaro, R. Smareglia, K. W. Smith, S. Taubenberger, O. Yaron, J. P. Anderson, C. Ashall, C. Balland, C. Baltay, C. Barbarino, F. E. Bauer, S. Baumont, D. Bersier, N. Blagorodnova, S. Bongard, M. T. Botticella, F. Bufano, M. Bulla, E. Cappellaro, H. Campbell, F. Cellier-Holzem, T.-W. Chen, M. J. Childress, A. Clocchiatti, C. Contreras, M. Dall'Ora, J. Danziger, T. de Jaeger, A. De Cia, M. D. Valle, M. Dennefeld, N. Elias-Rosa, N. Elman, U. Feindt, M. Fleury, E. Gall, S. Gonzalez-Gaitan, L. Galbany, A. M. Garoffolo, L. Greggio, L. L. Guillou, S. Hachinger, E. Hadjiyska, P. E. Hage, W. Hillebrandt, S. Hodgkin, E. Y. Hsiao, P. A. James, A. Jerkstrand, T. Kangas, E. Kankare, R. Kotak, M. Kromer, H. Kuncarayakti, G. Leloudas, P. Lundqvist, J. D. Lyman, I. M. Hook, K. Maguire, I. Manulis, S. J. Margheim, S. Mattila, J. R. Maund, P. A. Mazzali, M. Mc Crum, R. Mc Kinnon, M. E. Moreno-Raya, M. Nicholl, P. Nugent, R. Pain, G. Pignata, M. M. Phillips, J. Polshaw, M. L. Pumo, D. Rabinowitz, E. Reilly, C. Romero-Cañizales, R. Scalzo, B. Schmidt, S. Schulze, S. Sim, J. Sollerman, F. Taddia, L. Tartaglia, G. Terreran, L. Tomasella, M. Turatto, E. Walker, N. A. Walton, L. Wyrzykowski, F. Yuan, L. Zampieri, PESSTO: Survey description and products from the first data release by the Public ESO Spectroscopic Survey of Transient Objects. *Astron. Astrophys.* **579**, A40 (2015).
67. DESI Collaboration: Amir Aghamousa, J. Aguilar, S. Ahlen, S. Alam, L. E. Allen, C. A. Prieto, J. Annis, S. Bailey, C. Balland, O. Ballester, C. Baltay, L. Beaufore, C. Bebek, T. C. Beers, E. F. Bell, J. L. Bernal, R. Besuner, F. Beutler, C. Blake, H. Bleuler, M. Blomqvist, R. Blum, A. S. Bolton, C. Briceno, D. Brooks, J. R. Brownstein, E. Buckley-Geer, A. Burden, E. Burtin, N. G. Busca, R. N. Cahn, Y.-C. Cai, L. Cardiel-Sas, R. G. Carlberg, P.-H. Carton, R. Casas, F. J. Castander, J. L. Cervantes-Cota, T. M. Claybaugh, M. Close, C. T. Coker, S. Cole, J. Comparat, A. P. Cooper, M.-C. Cousinou, M. Crocce, J.-G. Cuby, D. P. Cunningham, T. M. Davis, K. S. Dawson, Axel de la Macorra, J. De Vicente, T. Delubac, M. Derwent, A. Dey, G. Dhungana, Z. Ding, P. Doel, Y. T. Duan, A. Ealet, J. Edelstein, S. Eftekharzadeh, D. J. Eisenstein, A. Elliott, S. Escoffier, M. Evatt, P. Fagrelius, X. Fan, K. Fanning, A. Farahi, J. Farihi, G. Favole, Y. Feng, E. Fernandez, J. R. Findlay, D. P. Finkbeiner, M. J. Fitzpatrick, B. Flaugher, S. Flender, A. Font-Ribera, J. E. Forero-Romero, P. Fosalba, C. S. Frenk, M. Fumagalli, B. T. Gaensicke, G. Gallo, J. Garcia-Bellido, E. Gaztanaga, Nicola Pietro Gentile Fusillo, T. Gerard, I. Gershkovich, T. Giannantonio, D. Gillet, Guillermo Gonzalez-de-Rivera, V. Gonzalez-Perez, S. Gott, O. Graur, G. Gutierrez, J. Guy, S. Habib, H. Heetderks, I. Heetderks, K. Heitmann, W. A. Hellwing, D. A. Herrera, S. Ho, S. Holland, K. Honscheid, E. Huff, T. A. Hutchinson, D. Huterer, H. S. Hwang, Joseph Maria Illa Laguna, Y. Ishikawa, D. Jacobs, N. Jeffrey, P. Jelinsky, E. Jennings, L. Jiang, J. Jimenez, J. Johnson, R. Joyce, E. Jullo, S. Juneau, S. Kama, A. Karcher, S. Karkar, R. Kehoe, N. Kennamer, S. Kent, M. Kilbinger, A. G. Kim, D. Kirkby, T. Kisner, E. Kitanidis, J.-P. Kneib, S. Koposov, E. Kovacs, K. Koyama, A. Kremin, R. Kron, L. Kronig, A. Kueter-Young, C. G. Lacey, R. Lafever, O. Lahav, A. Lambert, M. Lampton, M. Landriau, D. Lang, T. R. Lauer, Jean-Marc Le Goff, L. L. Guillou, Auguste Le Van Suu, J. H. Lee, S.-J. Lee, D. Leitner, M. Lesser, M. E. Levi, B. L'Huillier, B. Li, M. Liang, H. Lin, E. Linder, S. R. Loebman, Z. Lukić, J. Ma, N. M. Crann, C. Magneville, L. Makarem, M. Manera, C. J. Manser, R. Marshall, P. Martini, R. Massey, T. Matheson, J. M. Cauley, P. M. Donald, Ian D. Mc Greer, A. Meisner, N. Metcalfe, T. N. Miller, R. Miquel, J. Moustakas, A. Myers, M. Naik, J. A. Newman, R. C. Nichol, A. Nicola, Luiz Nicolati da Costa, J. Nie, G. Niz, P. Norberg, B. Nord, D. Norman, P. Nugent, T. O'Brien, M. Oh, K. A. G. Olsen, C. Padilla, H. Padmanabhan, N. Padmanabhan, N. Palanque-Delabrouille, A. Palmese, D. Pappalardo, I. Pâris, C. Park, A. Patej, J. A. Peacock, H. V. Peiris, X. Peng,

W. J. Percival, S. Perruchot, M. M. Pieri, R. Pogge, J. E. Pollack, C. Poppett, F. Prada, A. Prakash, R. G. Probst, D. Rabinowitz, A. Raichoor, C. H. Ree, A. Refregier, X. Regal, B. Reid, K. Reil, M. Rezaie, C. M. Rockosi, N. Roe, S. Ronayette, A. Roodman, A. J. Ross, N. P. Ross, G. Rossi, E. Rozo, V. Ruhlmann-Kleider, E. S. Rykoff, C. Sabiu, L. Samushia, E. Sanchez, J. Sanchez, D. J. Schlegel, M. Schneider, M. Schubnell, A. Secroun, U. Seljak, H.-J. Seo, S. Serrano, A. Shafieloo, H. Shan, R. Sharples, M. J. Sholl, W. V. Shourt, J. H. Silber, D. R. Silva, M. M. Sirk, A. Slosar, A. Smith, G. F. Smoot, D. Som, Y.-S. Song, D. Sprayberry, R. Staten, A. Stefanik, G. Tarle, S. S. Tie, J. L. Tinker, R. Tojeiro, F. Valdes, O. Valenzuela, M. Valluri, M. Vargas-Magana, L. Verde, A. R. Walker, J. Wang, Y. Wang, B. A. Weaver, C. Weaverdyck, R. H. Wechsler, D. H. Weinberg, M. White, Q. Yang, C. Yeche, T. Zhang, G.-B. Zhao, Y. Zheng, X. Zhou, Z. Zhou, Y. Zhu, H. Zou, Y. Zu, The DESI experiment part I: science, targeting, and survey design. arXiv:1611.00036 (2016).

68. DESI Collaboration, B. Abareshi, J. Aguilar, S. Ahlen, S. Alam, D. M. Alexander, R. Alfarsy, L. Allen, C. A. Prieto, O. Alves, J. Ameel, E. Armengaud, J. Asorey, A. Aviles, S. Bailey, A. Balaguera-Antolínez, O. Ballester, C. Baltay, A. Bault, S. F. Beltran, B. Benavides, S. B. Zvi, A. Berti, R. Besuner, F. Beutler, D. Bianchi, C. Blake, P. Blanc, R. Blum, A. Bolton, S. Bose, D. Bramall, S. Brieden, A. Brodzeller, D. Brooks, C. Brownewell, E. Buckley-Geer, R. N. Cahn, Z. Cai, R. Canning, R. Capasso, A. C. Rosell, P. Carton, R. Casas, F. J. Castander, J. L. Cervantes-Cota, S. Chabanier, E. Chaussidon, C. Chuang, C. Circosta, S. Cole, A. P. Cooper, L. da Costa, M.-C. Cousinou, A. Cuceu, T. M. Davis, K. Dawson, R. de la Cruz-Noriega, A. de la Macorra, A. de Mattia, J. D. Costa, P. Demmer, M. Derwent, A. Dey, B. Dey, G. Dhungana, Z. Ding, C. Dobson, P. Doel, J. D.-M. Cann, J. Donaldson, K. Douglass, Y. Duan, P. Dunlop, J. Edelstein, S. Eftekharzadeh, D. J. Eisenstein, M. Enriquez-Vargas, S. Escoffier, M. Evatt, P. Fagrelius, X. Fan, K. Fanning, V. A. Fawcett, S. Ferraro, J. Ereza, B. Flaugher, A. Font-Ribera, J. E. Forero-Romero, C. S. Frenk, S. Fromenteau, B. T. Gänsicke, C. Garcia-Quintero, L. Garrison, E. Gaztañaga, F. Gerardi, H. Gil-Marín, S. G. A. Gontcho, A. X. Gonzalez-Morales, G. Gonzalez-de-Rivera, V. Gonzalez-Perez, C. Gordon, O. Graur, D. Green, C. Grove, D. Gruen, G. Gutierrez, J. Guy, C. Hahn, S. Harris, D. Herrera, H. K. Herrera-Alcantar, K. Honscheid, C. Howlett, D. Huterer, V. Iršič, M. Ishak, P. Jelinsky, L. Jiang, J. Jimenez, Y. P. Jing, R. Joyce, E. Jullo, S. Juneau, N. G. Karaçaylı, M. Karamanis, A. Karcher, T. Karim, R. Kehoe, S. Kent, D. Kirkby, T. Kisner, F. Kitaura, S. E. Koposov, A. Kovács, A. Kremin, A. Krolewski, B. L'Huillier, O. Lahav, A. Lambert, C. Lamman, T.-W. Lan, M. Landriau, S. Lane, D. Lang, J. U. Lange, J. Lasker, L. Le Guillou, A. Leauthaud, A. Le Van Suu, M. E. Levi, T. S. Li, C. Magneville, M. Manera, C. J. Manser, B. Marshall, P. Martini, W. M. Collam, P. M. Donald, A. M. Meisner, J. Mena-Fernández, J. Meneses-Rizo, M. Mezcua, T. Miller, R. Miquel, P. Montero-Camacho, J. Moon, J. Moustakas, E. Mueller, A. Muñoz-Gutiérrez, A. D. Myers, S. Nadathur, J. Najita, L. Napolitano, E. Neilsen, J. A. Newman, J. D. Nie, Y. Ning, G. Niz, P. Norberg, H. E. Noriega, T. O'Brien, A. Obuljen, N. Palanque-Delabrouille, A. Palmese, P. Zhiwei, D. Pappalardo, X. Peng, W. J. Percival, S. Perruchot, R. Pogge, C. Poppett, A. Porredon, F. Prada, J. Prochaska, R. Pucha, A. Pérez-Fernández, I. Pérez-Ràfols, D. Rabinowitz, A. Raichoor, S. Ramirez-Solano, C. Ramírez-Pérez, C. Ravoux, K. Reil, M. Rezaie, A. Rocher, C. Rockosi, N. A. Roe, A. Roodman, A. J. Ross, G. Rossi, R. Ruggeri, V. Ruhlmann-Kleider, C. G. Sabiu, S. Gaines, K. Said, A. Saintonge, J. S. Catonga, L. Samushia, E. Sanchez, C. Saulder, E. Schaan, E. Schlafly, D. Schlegel, J. Schmoll, D. Scholte, M. Schubnell, A. Secroun, H. Seo, S. Serrano, R. M. Sharples, M. J. Sholl, J. H. Silber, D. R. Silva, M. Sirk, M. Siudek, A. Smith, D. Sprayberry, R. Staten, B. Stupak, T. Tan, G. Tarlé, S. S. Tie, R. Tojeiro, L. A. Ureña-López, F. Valdes, O. Valenzuela, M. Valluri, M. Vargas-Magaña, L. Verde, M. Walther, B. Wang, M. S. Wang, B. A. Weaver, C. Weaverdyck, R. Wechsler, M. J. Wilson, J. Yang, Y. Yu, S. Yuan, C. Yèche, H. Zhang, K. Zhang, C. Zhao, R. Zhou, Z. Zhou, H. Zou, J. Zou, S. Zou, Y. Zu, Overview of the instrumentation for the Dark Energy Spectroscopic Instrument. *Astron. Astrophys.* **164**, 207 (2022).

69. C. H. Hahn, M. J. Wilson, O. Ruiz-Macias, S. Cole, D. H. Weinberg, J. Moustakas, A. Kremin, J. L. Tinker, A. Smith, R. H. Wechsler, S. Ahlen, S. Alam, S. Bailey, D. Brooks, A. P. Cooper, T. M. Davis, K. Dawson, A. Dey, B. Dey, S. Eftekharzadeh, D. J. Eisenstein, K. Fanning, J. E. Forero-Romero, C. S. Frenk, E. Gaztañaga, S. G. A. Gontcho, J. Guy, K. Honscheid, M. Ishak, S. Juneau, R. Kehoe, T. Kisner, T.-W. Lan, M. Landriau, L. L. Guillou, M. E. Levi, C. Magneville, P. Martini, A. Meisner, A. D. Myers, J. Nie, P. Norberg, N. Palanque-Delabrouille, W. J. Percival, C. Poppett, F. Prada, A. Raichoor, A. J. Ross, S. Gaines, C. Saulder, E. Schlafly, D. Schlegel, D. Sierra-Porta, G. Tarle, B. A. Weaver, C. Yèche, P. Zarrouk, R. Zhou, Z. Zhou, H. Zou, The DESI bright galaxy survey: Final target selection, design, and validation. *Astrophys. J.* **165**, 253 (2023).

70. A. Dey, D. J. Schlegel, D. Lang, R. Blum, K. Burleigh, X. Fan, J. R. Findlay, D. Finkbeiner, D. Herrera, S. Juneau, M. Landriau, M. Levi, I. M. Greer, A. Meisner, A. D. Myers, J. Moustakas, P. Nugent, A. Patej, E. F. Schlafly, A. R. Walker, F. Valdes, B. A. Weaver, C. Yèche, H. Zou, X. Zhou, B. Abareshi, T. M. C. Abbott, B. Abolfathi, C. Aguilera, S. Alam, L. Allen, A. Alvarez, J. Annis, B. Ansarinejad, M. Aubert, J. Beechert, E. F. Bell, S. Y. Ben Zvi, F. Beutler, R. M. Bielby, A. S. Bolton, C. Briceño, E. J. Buckley-Geer, K. Butler, A. Calamida, R. G. Carlberg, P. Carter, R. Casas, F. J. Castander, Y. Choi, J. Comparat, E. Cukanovaite, T. Delubac, K. De Vries, S. Dey, G. Dhungana, M. Dickinson, Z. Ding, J. B. Donaldson, Y. Duan, C. J. Duckworth, S. Eftekharzadeh, D. J. Eisenstein, T. Etourneau, P. A. Fagrelius, J. Farihi, M. Fitzpatrick, A. Font-Ribera, L. Fulmer, B. T. Gänsicke, E. Gaztanaga, K. George, D. W. Gerdes, S. G. A. Gontcho, C. Gorgoni, G. Green, J. Guy, D. Harmer, M. Hernandez, K. Honscheid, L. Huang, D. J. James, B. T. Jannuzi, L. Jiang, R. Joyce, A. Karcher, S. Karkar, R. Kehoe, Jean-Paul, Kneib, A. Kueter-Young, T.-W. Lan, T. R. Lauer, L. L. Guillou, A. Le Van Suu, J. H. Lee, M. Lesser, L. P. Levasseur, T. S. Li, J. L. Mann, R. Marshall, C. E. Martínez-Vázquez, P. Martini, H. du Mas des Bourboux, S. M. Manus, T. G. Meier, B. Ménard, N. Metcalfe, A. Muñoz-Gutiérrez, J. Najita, K. Napier, G. Narayan, J. A. Newman, J. Nie, B. Nord, D. J. Norman, K. A. G. Olsen, A. Paat, N. Palanque-Delabrouille, X. Peng, C. L. Poppett, M. R. Poremba, A. Prakash, D. Rabinowitz, A. Raichoor, M. Rezaie, A. N. Robertson, N. A. Roe, A. J. Ross, N. P. Ross, G. Rudnick, S. Gaines, A. Saha, F. J. Sánchez, E. Savary, H. Schweiker, A. Scott, H.-J. Seo, H. Shan, D. R. Silva, Z. Slepian, C. Soto, D. Sprayberry, R. Staten, C. M. Stillman, R. J. Stupak, D. L. Summers, S. S. Tie, H. Tirado, M. Vargas-Magaña, A. K. Vivas, R. H. Wechsler, D. Williams, J. Yang, Q. Yang, T. Yapici, D. Zaritsky, A. Zenteno, K. Zhang, T. Zhang, R. Zhou, Z. Zhou, Overview of the DESI legacy imaging surveys. *Astrophys. J.* **157**, 168 (2019).

71. H. Zou, X. Zhou, X. Fan, T. Zhang, Z. Zhou, J. Nie, X. Peng, I. M. Greer, L. Jiang, A. Dey, D. Fan, B. He, Z. Jiang, D. Lang, M. Lesser, J. Ma, S. Mao, D. Schlegel, J. Wang, Project overview of the Beijing-Arizona Sky Survey. *Publ. Astron. Soc. Pac.* **129**, 064101 (2017).

72. J. Guy, S. Bailey, A. Kremin, S. Alam, D. M. Alexander, C. Allende Prieto, S. Ben Zvi, A. S. Bolton, D. Brooks, E. Chaussidon, A. P. Cooper, K. Dawson, A. de la Macorra, A. Dey, B. Dey, G. Dhungana, D. J. Eisenstein, A. Font-Ribera, J. E. Forero-Romero, E. Gaztañaga, S. G. A. Gontcho, D. Green, K. Honscheid, M. Ishak, R. Kehoe, D. Kirkby, T. Kisner, S. E. Koposov, T.-W. Lan, M. Landriau, L. Le Guillou, M. E. Levi, C. Magneville, C. J. Manser, P. Martini, A. M. Meisner, R. Miquel, J. Moustakas, A. D. Myers, J. A. Newman, J. Nie, N. Palanque-Delabrouille, W. J. Percival, C. Poppett, F. Prada, A. Raichoor, C. Ravoux, A. J. Ross, E. F. Schlafly, D. Schlegel, M. Schubnell, R. M. Sharples, G. Tarlé, B. A. Weaver, C. Yéche, R. Zhou, Z. Zhou, H. Zou, The spectroscopic data processing pipeline for the Dark Energy Spectroscopic Instrument. *Astrophys. J.* **165**, 144 (2023).

73. P. A. Evans, A. P. Beardmore, K. L. Page, L. G. Tyler, J. P. Osborne, M. R. Goad, P. T. O'Brien, L. Vetere, J. Racusin, D. Morris, D. N. Burrows, M. Capalbi, M. Perri, N. Gehrels, P. Romano, An online repository of *Swift*/XRT light curves of γ-ray bursts. *Astrophys. J.* **469**, 379–385 (2007).

74. P. A. Evans, A. P. Beardmore, K. L. Page, J. P. Osborne, P. T. O'Brien, R. Willingale, R. L. C. Starling, D. N. Burrows, O. Godet, L. Vetere, J. Racusin, M. R. Goad, K. Wiersema, L. Angelini, M. Capalbi, G. Chincarini, N. Gehrels, J. A. Kennea, R. Margutti, D. C. Morris, C. J. Mountford, C. Pagani, M. Perri, P. Romano, N. Tanvir, Methods and results of an automatic analysis of a complete sample of Swift-XRT observations of GRBs. *Mon. Not. R. Astron. Soc.* **397**, 1177–1201 (2009).

75. W. Cash, Parameter estimation in astronomy through application of the likelihood ratio. *Astrophys. J.* **228**, 939–947 (1979).

76. P. Predehl, R. Andritschke, V. Arefiev, V. Babyshkin, O. Batanov, W. Becker, H. Böhringer, A. Bogomolov, T. Boller, K. Borm, W. Bornemann, H. Bräuninger, M. Brüggen, H. Brunner, M. Brusa, E. Bulbul, M. Buntov, V. Burwitz, W. Burkert, N. Clerc, E. Churazov, D. Coutinho, T. Dauser, K. Dennerl, V. Doroshenko, J. Eder, V. Emberger, T. Eraerds, A. Finoguenov, M. Freyberg, P. Friedrich, S. Friedrich, M. Fürmetz, A. Georgakakis, M. Gilfanov, S. Granato, C. Grossberger, A. Gueguen, P. Gureev, F. Haberl, O. Hälker, G. Hartner, G. Hasinger, H. Huber, L. Ji, A. v. Kienlin, W. Kink, F. Korotkov, I. Kreykenbohm, G. Lamer, I. Lomakin, I. Lapshov, T. Liu, C. Maitra, N. Meidinger, B. Menz, A. Merloni, T. Mernik, B. Mican, J. Mohr, S. Müller, K. Nandra, V. Nazarov, F. Pacaud, M. Pavlinsky, E. Perinati, E. Pfeffermann, D. Pietschner, M. E. Ramos-Ceja, A. Rau, J. Reiffers, T. H. Reiprich, J. Robrade, M. Salvato, J. Sanders, A. Santangelo, M. Sasaki, H. Scheuerle, C. Schmid, J. Schmitt, A. Schwope, A. Shirshakov, M. Steinmetz, I. Stewart, L. Strüder, R. Sunyaev, C. Tenzer, L. Tiedemann, J. Trümper, V. Voron, P. Weber, J. Wilms, V. Yaroshenko, The eROSITA X-ray telescope on SRG. *Astron. Astrophys.* **647**, A1 (2021).

77. J. P. McMullin, B. Waters, D. Schiebel, W. Young, K. Golap, "CASA architecture and applications," in *Astronomical Data Analysis Software and Systems XVI*, R. A. Shaw, F. Hill, D. J. Bell, Eds., vol. 376 of *Astronomical Society of the Pacific Conference Series* (Astronomical Society of the Pacific, 2007), p. 127.

78. THE CASA TEAM, B. Bean, S. Bhatnagar, S. Castro, J. D. Meyer, B. Emonts, E. Garcia, R. Garwood, K. Golap, J. G. Villalba, P. Harris, Y. Hayashi, J. Hoskins, M. Hsieh, P. Jagannathan, W. Kawasaki, A. Keimpema, M. Kettenis, J. Lopez, J. Marvil, J. Masters, A. M. Nichols, D. Mehringer, R. Miel, G. Moellenbrock, F. Montesino, T. Nakazato, J. Ott, D. Petry, M. Pokorny, R. Raba, U. Rau, D. Schiebel, N. Schweighart, S. Sekhar, K. Shimada, D. Small, J.-W. Steeb, K. Sugimoto, V. Suoranta, T. Tsutsumi, I. M. van Bemmel, M. Verkouter, A. Wells, W. Xiong, A. Szomoru, M. Griffith, B. Glendenning, J. Kern, CASA, the Common Astronomy Software Applications for Radio Astronomy. *Publ. Astron. Soc. Pac.* **134**, 114501 (2022).

79. D. S. Briggs, *High Fidelity Interferometric Imaging: Robust Weighting and NNLS Deconvolution*, vol. 187 of *American Astronomical Society Meeting Abstracts* (American Astronomical Society, 1995).

80. J. Moldon, "eMCP: e-MERLIN CASA pipeline" (Astrophysics Source Code Library, record ascl:2109.006, 2021).

81. E. W. Greisen, "AIPS, the VLA, and the VLBA," in *Information Handling in Astronomy - Historical Vistas*, A. Heck, Ed., vol. 285 of *Astrophysics and Space Science Library* (Springer, 2003), p. 109.
82. A. J. Beasley, J. E. Conway, VLBI Phase-Referencing, in *Very Long Baseline Interferometry and the VLBA*, J. A. Zensus, P. J. Diamond, P. J. Napier, Eds., vol. 82 of *Astronomical Society of the Pacific Conference Series* (Astronomical Society of the Pacific, 1995), p. 327.
83. M. C. Shepherd, T. J. Pearson, G. B. Taylor, *DIFMAP: An Interactive Program for Synthesis Imaging* (American Astronomical Society, 1994), vol. 26.
84. K. A. Arnaud, "XSPEC: The first ten years," in *Astronomical Data Analysis Software and Systems V*, G. H. Jacoby, J. Barnes, Eds., vol. 101 of *Astronomical Society of the Pacific Conference Series* (Astronomical Society of the Pacific, 1996), p. 17.
85. HI4PI Collaboration, HI4PI: A full-sky H I survey based on EBHIS and GASS. *Astron. Astrophys.* **594**, A116 (2016).
86. J. Wilms, A. Allen, R. McCray, On the absorption of X-rays in the interstellar medium. *Astrophys. J.* **542**, 914–924 (2000).
87. D. A. Verner, G. J. Ferland, K. T. Korista, D. G. Yakovlev, Atomic data for astrophysics. II. New analytic FITS for photoionization cross sections of atoms and ions. *Astrophys. J.* **465**, 487 (1996).
88. Z. Lin, Y. Wang, D.-F. Bu, J. Mao, J. Liu, Delayed launch of ultrafast outflows in the tidal disruption event AT2020afhd. *Astrophys. J.* **989**, L9 (2025).
89. Y. Wang, R. D. Baldi, S. del Palacio, M. Guolo, X. Yang, Y. Zhang, C. Done, N. C. Segura, D. R. Pasham, M. Middleton, D. Altamirano, P. Gandhi, E. Qiao, N. Jiang, H. Yan, M. Giroletti, G. Migliori, I. M. Hardy, F. Panessa, C. Jin, R. Shen, L. Dai, The radio detection and accretion properties of the peculiar nuclear transient AT 2019avd. *Mon. Not. R. Astron. Soc.* **520**, 2417–2435 (2023).
90. J. Granot, R. Sari, The shape of spectral breaks in gamma-ray burst afterglows. *Astrophys. J.* **568**, 820–829 (2002).
91. Y. Cendes, E. Berger, K. D. Alexander, R. Chornock, R. Margutti, B. Metzger, M. H. Wieringa, M. F. Bietenholz, A. Hajela, T. Laskar, M. C. Stroh, G. Terreran, Ubiquitous late radio emission from tidal disruption events. *Astrophys. J.* **971**, 185 (2024).
92. G. Ashton, M. Hübner, P. D. Lasky, C. Talbot, K. Ackley, S. Biscoveanu, Q. Chu, A. Divakarla, P. J. Easter, B. Goncharov, BILBY: A user-friendly Bayesian inference library for gravitational-wave astronomy. *Astrophys. J. Suppl. Ser.* **241**, 27 (2019).
93. D. Foreman-Mackey, D. W. Hogg, D. Lang, J. Goodman, emcee: The MCMC hammer. *Publ. Astron. Soc. Pac.* **125**, 306–312 (2013).
94. R. Barniol Duran, E. Nakar, T. Piran, Radius constraints and minimal equipartition energy of relativistically moving synchrotron sources. *Astrophys. J.* **772**, 78 (2013).
95. T. Matsumoto, T. Piran, Generalized equipartition method from an arbitrary viewing angle. *Mon. Not. R. Astron. Soc.* **522**, 4565–4576 (2023).
96. G. Bruzual, S. Charlot, Stellar population synthesis at the resolution of 2003. 344, 1000–1028 (2003).
97. D. Calzetti, L. Armus, R. C. Bohlin, A. L. Kinney, J. Koornneef, T. Storchi-Bergmann, The dust content and opacity of actively star-forming galaxies. *Astrophys. J.* **533**, 682–695 (2000).
98. B. T. Draine, G. Aniano, O. Krause, B. Groves, K. Sandstrom, R. Braun, A. Leroy, U. Klaas, H. Linz, H.-W. Rix, E. Schinnerer, A. Schmiedeke, F. Walter, Andromeda's dust. *Astrophys. J.* **780**, 172 (2014).
99. J. Fritz, A. Franceschini, E. Hatziminaoglou, Revisiting the infrared spectra of active galactic nuclei with a new torus emission model. *Mon. Not. R. Astron. Soc.* **366**, 767–786 (2006).
100. M. Cappellari, E. Emsellem, Parametric recovery of line-of-sight velocity distributions from absorption-line spectra of galaxies via penalized likelihood. *Publ. Astron. Soc. Pac.* **116**, 138–147 (2004).
101. M. Cappellari, Improving the full spectrum fitting method: Accurate convolution with Gauss-Hermite functions. *Mon. Not. R. Astron. Soc.* **466**, 798–811 (2017).
102. P. Sánchez-Blázquez, R. F. Peletier, J. Jiménez-Vicente, N. Cardiel, A. J. Cenarro, J. Falcón-Barroso, J. Gorgas, S. Selam, A. Vazdekis, Medium-resolution Isaac Newton Telescope library of empirical spectra. *Mon. Not. R. Astron. Soc.* **371**, 703–718 (2006).
103. P. Du, PuDu-Astro/DASpec: DASpec: A code for spectral decomposition of active galactic nuclei, version v0.8.1, Zenodo (2024).
104. J. E. Greene, L. C. Ho, Estimating black hole masses in active galaxies using the Hα emission line. *Astrophys. J.* **630**, 122–129 (2005).
105. J. Kormendy, L. C. Ho, Coevolution (Or Not) of supermassive black holes and host galaxies. *Annu. Rev. Astron. Astrophys.* **51**, 511–653 (2013).
106. N. J. McConnell, C.-P. Ma, Revisiting the scaling relations of black hole masses and host galaxy properties. *Astrophys. J.* **764**, 184 (2013).
107. R. J. McLure, M. J. Jarvis, Measuring the black hole masses of high-redshift quasars. *Mon. Not. R. Astron. Soc.* **337**, 109–116 (2002).
108. M. Vestergaard, B. M. Peterson, Determining central black hole masses in distant active galaxies and quasars. II. Improved optical and UV scaling relationships. *Astrophys. J.* **641**, 689–709 (2006).
109. Y. Shen, J. E. Greene, L. C. Ho, W. N. Brandt, K. D. Denney, K. Horne, L. Jiang, C. S. Kochanek, I. D. McGreer, A. Merloni, The Sloan Digital Sky Survey Reverberation Mapping project: No evidence for evolution in the $M_\bullet$–σ_* relation to z~1. *Astrophys. J.* **805**, 96 (2015).
110. J. H. Krolik, T. Piran, Jets from tidal disruptions of stars by black holes. *Astrophys. J.* **749**, 92 (2012).
111. L. E. Strubbe, E. Quataert, Optical flares from the tidal disruption of stars by massive black holes. *Mon. Not. R. Astron. Soc.* **400**, 2070–2084 (2009).
112. J. M. Bardeen, W. H. Press, S. A. Teukolsky, Rotating black holes: Locally nonrotating frames, energy extraction, and scalar synchrotron radiation. *Astrophys. J.* **178**, 347–370 (1972).
113. P. C. Fragile, O. M. Blaes, P. Anninos, J. D. Salmonson, Global general relativistic magnetohydrodynamic simulation of a tilted black hole accretion disk. *Astrophys. J.* **668**, 417–429 (2007).
114. M. R. Bate, I. A. Bonnell, C. J. Clarke, S. H. Lubow, G. I. Ogilvie, J. E. Pringle, C. A. Tout, Observational implications of precessing protostellar discs and jets. *Mon. Not. R. Astron. Soc.* **317**, 773–781 (2000).
115. F. Panessa, R. D. Baldi, A. Laor, P. Padovani, E. Behar, I. McHardy, The origin of radio emission from radio-quiet active galactic nuclei. *Nat. Astron.* **3**, 387–396 (2019).
116. W.-H. Lei, B. Zhang, H. Gao, Frame dragging, disk warping, jet precessing, and dipped X-ray light curve of Sw J1644+57. *Astrophys. J.* **762**, 98 (2013).
117. H. K. Lee, R. A. M. J. Wijers, G. E. Brown, The Blandford-Znajek process as a central engine for a gamma-ray burst. *Phys. Rep.* **325**, 83–114 (2000).
118. W.-H. Lei, B. Zhang, Black hole spin in Sw J1644+57 and Sw J2058+05. *Astrophys. J. Lett.* **740**, L27 (2011).
119. M. Livio, G. I. Ogilvie, J. E. Pringle, Extracting energy from black holes: The relative importance of the Blandford-Znajek mechanism. *Astrophys. J.* **512**, 100–104 (1999).

Acknowledgments: We thank the NICER, Swift, XMM-Newton, VLA, ATCA, e-MERLIN, and VLBA teams for approving our ToO/DDT requests. The National Radio Astronomy Observatory is a facility of the National Science Foundation (NSF) operated under cooperative agreement by Associated Universities Inc. The Australia Telescope Compact Array is part of the Australia Telescope National Facility (grid.421683.a), which is funded by the Australian Government for operation as a National Facility managed by CSIRO. We acknowledge the Gomeroi people as the traditional owners of the Observatory site. e-MERLIN is a National Facility operated by the University of Manchester at Jodrell Bank Observatory on behalf of STFC, part of UK Research and Innovation. : This research used data obtained with the Dark Energy Spectroscopic Instrument (DESI). DESI construction and operations is managed by the Lawrence Berkeley National Laboratory. This material is based upon work supported by the US Department of Energy, Office of Science, Office of High-Energy Physics, under contract no. DE-AC02-05CH11231, and by the National Energy Research Scientific Computing Center, a DOE Office of Science User Facility under the same contract. Additional support for DESI was provided by the US NSF, Division of Astronomical Sciences under contract no. AST-0950945 to the NSF's National Optical-Infrared Astronomy Research Laboratory; the Science and Technology Facilities Council of the United Kingdom; the Gordon and Betty Moore Foundation; the Heising-Simons Foundation; the French Alternative Energies and Atomic Energy Commission (CEA); the National Council of Science and Technology of Mexico (CONACYT); the Ministry of Science and Innovation of Spain (MICINN); and the DESI Member Institutions: www.desi.lbl.gov/collaborating-institutions. The DESI collaboration is honored to be permitted to conduct scientific research on Iolkam Du'ag (Kitt Peak), a mountain with particular significance to the Tohono O'odham Nation. Any opinions, findings, and conclusions or recommendations expressed in this material are those of the authors and do not necessarily reflect the views of the US NSF, the US Department of Energy, or any of the listed funding agencies. : This study used observations collected at the European Organisation for Astronomical Research in the Southern Hemisphere, Chile, as part of ePESSTO+ (the advanced Public ESO Spectroscopic Survey for Transient Objects Survey). ePESSTO+ observations were obtained under ESO program ID 112.25JQ. : We thank P. Du for coordinating the Lijiang 2.4m Telescope observations, which provided two spectra taken on 24 February 2024. We also thank N. Jiang, W. Zhang, Y. Lu, S. Wang, and J. Wang for the helpful discussions and W. Jiang for help with the VLBA data analysis. **Funding:** This research was supported by the National Natural Science Foundation of China (NSFC) under grant nos. 12588202, 12173103, 12261141691, 12473012, and 12203041; by the New Cornerstone Science Foundation through the New Cornerstone Investigator Program and the XPLORER PRIZE; by the Strategic Priority Program of the Chinese Academy of Sciences under grant nos. XDB41000000 and XDB0550203; by ANID, Millennium Science Initiative, ICN12_009; and by a research grant (VIL60862) from VILLUM FONDEN. S.d.P. acknowledges support from ERC Advanced grant 789410. P.C. acknowledges support via Research Council of Finland (grant 340613). S.-N.Z. acknowledges support from the NSFC (grant no. 12333007). M.N. is supported by the European Research Council (ERC) under the European Union's Horizon 2020 research and innovation programme (grant agreement no. 948381) and by UK Space Agency grant no. ST/Y000692/1. T.P. acknowledges the financial support from the Slovenian Research Agency (grants I0-0033, P1-0031, J1-8136, J1-2460, and Z1-1853). H.Z. acknowledges National Key R&D Program of China (grant nos. 2023YFA1607804, 2022YFA1602902, and 2023YFA1608100) and NSFC (grant nos. 12120101003, 12373010, and 12233008). L.G. acknowledges financial support from AGAUR, CSIC, MCIN, and AEI 10.13039/501100011033 under projects PID2023-151307NB-I00, PIE 20215AT016, CEX2020-001058-M, ILINK23001, COOPB2304, and 2021-SGR-01270. C.P.G. acknowledges financial support from the Secretary of Universities and Research (Government of Catalonia) and by the Horizon 2020 Research and Innovation Programme of the European Union under the Marie Skłodowska-Curie and the Beatriu de Pinós 2021 BP 00168 programme, from the Spanish Ministerio de Ciencia e Innovación (MCIN) and the Agencia Estatal de Investigación (AEI) 10.13039/501100011033 under the PID2023-151307NB-I00 SNNEXT project, from Centro Superior de Investigaciones Científicas (CSIC) under the PIE project 20215AT016 and the program Unidad de Excelencia María de Maeztu CEX2020-001058-M, and from the Departament de Recerca i Universitats de la Generalitat de Catalunya through the 2021-SGR-01270 grant. M.P.-T. acknowledges financial support from the Severo Ochoa grant CEX2021-001131-S and from the Spanish grant PID2023-147883NB-C21, funded by MCIU/AEI/10.13039/501100011033, as well as support through ERDF/EU. T.-W.C. acknowledges the Yushan Fellow Program by the Ministry of Education, Taiwan, for the financial support (MOE-111-YSFMS-0008-001-P1). F.-G.X. and L.W. were supported, in part, by National SKA Program of China (grant nos. 2020SKA0110100 and 2020SKA0110200) and by NSFC (grant nos. 12373017, 12192220, and 12192223). F.O. acknowledges support from MIUR, PRIN 2020 (grant 2020KB33TP) "Multimessenger astronomy in the Einstein Telescope Era (METE)" and from INAF-MINIGRANT (2023): "SeaTiDE - Searching for Tidal Disruption Events with ZTF: the Tidal Disruption Event population in the era of wide field surveys." **Author contributions:** Conceptualization: Y.W., W.-H.L., S.-N.Z., J.-F.L., S.d.P., R.D.B., A.Y., X.C., E.Q., X.S., F.O., and D.A. Methodology: Y.W., Z.L., W.-H.L., S.-N.Z., L.J., J.-F.L., B.Z., F.-G.X., D.B., D.R.P., S.d.P., A.Y., and D.A. Software: Y.W., Z.L., L.W., W.-H.L., S.d.P., Y.H., and A.Y. Validation: Y.W., Z.L., L.W., W.-H.L., Y.H., A.Y., P.C., Y.Z., W.L., H.W., T.E.M.-B., and J.-Y.W. Formal analysis: Y.W., Z.L., L.W., W.-H.L., L.J., F.-G.X., Y.H., A.Y., R.-R.C., Y.Z., X.C., H.W., D.R.A.W.-B., and Z.-H.Y. Investigation: Y.W., Z.L., W.-H.L., S.d.P., R.D.B., L.Y., Z.-H.Y., F.-G.X., D.B., X.C., H.F., Y.H., A.Y., A.-L.W., P.C., D.R.A.W.-B., W.L., M.N., G.L., C.P.G., T.P., T.W., J.-Y.W., W.-J.G., L.G., and T.-W.C. Resources: Y.W., L.W., Y.H., A.Y., J.W., H.Z., W.-J.G., G.L., J.P.A., T.E.M.-B., Y.-L.Q., C.I., T.P., L.G., and T.-W.C. Data curation: Y.W., Z.L., L.W., S.W., A.Y., L.Y., A.-L.W., Y.Z., Z.-H.Y., J.W., G.L., W.-J.G., C.I., J.P.A., M.G., and T.P. Writing—original draft: Y.W., Z.L., L.W., W.-H.L., L.J., J.-F.L., S.d.P., R.D.B., D.B., Z.-H.Y., and H.Z. Writing—reviewing and editing: Y.W., Z.L., L.W., W.-H.L., L.J., S.-N.Z., J.-F.L., F.-G.X., D.B., H.F., S.d.P., X.S., R.D.B., Y.H., A.Y., P.C., D.R.A.W.-B., G.L., J.P.A., M.N., L.M., T.E.M.-B., C.P.G., T.W., M.G., F.O., D.A., L.G., M.P.-T., and T.-W.C. Visualization: Y.W., Z.L., L.W., W.-H.L., S.d.P., R.D.B., J.-Y.W., and P.C. Supervision: Y.W., W.-H.L., and J.-F.L. Project administration: Y.W., J.-F.L., and J.P.A. Funding acquisition: Y.W., W.-H.L., J.-F.L., and C.I. **Competing interests:** The authors declare that they have no competing interests. **Data and materials availability:** All data needed to evaluate the conclusions in the paper are present in the paper and/or the Supplementary Materials. The data used to generate Figs. 1, 2, 3, and 5, along with the Python codes for the LSP and CCF, are available on Zenodo (https://doi.org/10.5281/zenodo.14195067).

Submitted 10 May 2025
Accepted 22 October 2025
Published 10 December 2025
10.1126/sciadv.ady9068